



OPEN ACCESS

Edited by:

Jing-Ning Zhu,
Nanjing University, China

Reviewed by:

Lyandysha Zholudeva,
Drexel University, United States
Tuan Vu Bui,
University of Ottawa, Canada

***Correspondence:**

Frédéric Clotman
frederic.clotman@uclouvain.be

† Present address:

Maria Hidalgo-Figueroa,
Neuropsychopharmacology
and Psychobiology Research Group,
Area of Psychobiology, Department
of Psychology, University of Cádiz,
Cádiz, Spain;
Instituto de Investigación e Innovación
en Ciencias Biomédicas de Cádiz
(INIBICA), Cádiz, Spain
Cédric Francius,
PAREXEL International, Paris, France

Specialty section:

This article was submitted to
Cellular Neurophysiology,
a section of the journal
Frontiers in Cellular Neuroscience

Received: 14 January 2019

Accepted: 12 April 2019

Published: 05 June 2019

Citation:

Harris A, Masgutova G, Collin A,
Toch M, Hidalgo-Figueroa M,
Jacob B, Corcoran LM, Francius C
and Clotman F (2019) *Onecut Factors
and Pou2f2 Regulate the Distribution
of V2 Interneurons in the Mouse
Developing Spinal Cord.*
Front. Cell. Neurosci. 13:184.
doi: 10.3389/fncel.2019.00184

Onecut Factors and Pou2f2 Regulate the Distribution of V2 Interneurons in the Mouse Developing Spinal Cord

Audrey Harris¹, Gauhar Masgutova¹, Amandine Collin¹, Mathilde Toch¹,
Maria Hidalgo-Figueroa^{1†}, Benvenuto Jacob², Lynn M. Corcoran³, Cédric Francius^{1†} and
Frédéric Clotman^{1*}

¹ Laboratory of Neural Differentiation, Institute of Neuroscience, Université catholique de Louvain, Brussels, Belgium,

² Institute of Neuroscience, System and Cognition Division, Université catholique de Louvain, Brussels, Belgium, ³ Molecular Immunology Division and Immunology Division, The Walter and Eliza Hall Institute of Medical Research, Parkville, VIC, Australia

Acquisition of proper neuronal identity and position is critical for the formation of neural circuits. In the embryonic spinal cord, cardinal populations of interneurons diversify into specialized subsets and migrate to defined locations within the spinal parenchyma. However, the factors that control interneuron diversification and migration remain poorly characterized. Here, we show that the *Onecut* transcription factors are necessary for proper diversification and distribution of the V2 interneurons in the developing spinal cord. Furthermore, we uncover that these proteins restrict and moderate the expression of spinal isoforms of *Pou2f2*, a transcription factor known to regulate B-cell differentiation. By gain- or loss-of-function experiments, we show that *Pou2f2* contribute to regulate the position of V2 populations in the developing spinal cord. Thus, we uncovered a genetic pathway that regulates the diversification and the distribution of V2 interneurons during embryonic development.

Keywords: embryonic spinal cord, V2 interneurons, *Onecut*, *Pou2f2*, neuronal migration, differentiation

INTRODUCTION

Neuronal migration is a critical feature of CNS development. It enables neurons to reach an adequate location in the nervous parenchyma and to properly integrate into neural circuits. The mechanisms that regulate neuronal migration have been extensively studied in the developing brain, particularly for cortical interneurons (INs) (Guo and Anton, 2014; Barber and Pierani, 2016). In contrast, the factors that control IN migration in the developing spinal cord remain almost totally unknown.

In the embryonic spinal cord, distinct neuronal populations are generated from different progenitor domains orderly distributed along the dorso-ventral axis of the ventricular zone. These progenitors produce motor neurons and multiple populations of ventral or dorsal INs

(Lu et al., 2015; Lai et al., 2016). Although spinal IN populations do not organize into columns along the anteroposterior axis of the spinal cord, they each migrate according to a stereotyped pattern and settle down at specific focused or diffuse locations in the spinal parenchyma (Grossmann et al., 2010). Recent studies demonstrated that proper neuronal distribution is critical for adequate formation of spinal circuits. Indeed, the clustering and dorso-ventral settling position of motor neuron pools critically pattern sensory input specificity (Surmeli et al., 2011). Position of dorsal INs along the medio-lateral axis in lamina V determines their connectivity with sensory afferents (Hilde et al., 2016) while extensor and flexor premotor INs segregate along the medio-lateral axis of the spinal cord (Tripodi et al., 2011). Positional distinctions among premotor INs additionally correlate with their output to different motor columns (Goetz et al., 2015) and differential distribution of V1 IN subsets constrain patterns of input from sensory and from motor neurons (Bikoff et al., 2016). Consistently, distinct ventral IN subsets are differentially distributed along the anteroposterior axis of the spinal cord (Francius et al., 2013; Bikoff et al., 2016; Hayashi et al., 2018) and integrate into specific local microcircuit modules (Hayashi et al., 2018). However, the molecular mechanisms that regulate proper distribution of spinal INs remain elusive.

During their migration, cardinal populations of spinal neurons undergo progressive diversification into distinct subsets that exert specific functions in spinal circuits (Catela et al., 2015; Lu et al., 2015; Lai et al., 2016). For example, V2 INs divide into major V2a and V2b and minor V2c and V2d populations characterized by the expression of *Chx10*, *Gata3*, *Sox1*, and *Shox2*, respectively. V2a and V2d are excitatory neurons that participate in left–right alternation at high speed and contribute to rhythmic activation of locomotor circuits, respectively (Crone et al., 2008; Dougherty and Kiehn, 2010; Dougherty et al., 2013). V2b cells are inhibitory INs that participate in alternation of flexor vs. extensor muscle contraction (Britz et al., 2015). As observed for V1 INs (Bikoff et al., 2016), V2 cells further diversify into more discrete subpopulations differentially distributed along the anteroposterior axis of the spinal cord (Francius et al., 2013; Hayashi et al., 2018). However, specific functions of these IN subsets have not been investigated yet, and the mechanisms that govern their production remain currently unknown.

Recently, we identified *Onecut* (OC) transcription factors as regulators of neuronal diversification (Roy et al., 2012; Francius and Clotman, 2014; Kabayiza et al., 2017) and of dorsal IN migration (Kabayiza et al., 2017) in the developing spinal cord. OC factors, namely Hepatocyte Nuclear Factor-6 (HNF-6, or OC-1), OC-2, and OC-3, are transcriptional activators present in the digestive tract and in the CNS during embryonic development (Lemaigre et al., 1996; Landry et al., 1997; Jacquemin et al., 1999; Vanhorenbeeck et al., 2002; Jacquemin et al., 2003b). In neural tissue, they regulate production (España and Clotman, 2012a), diversification (Roy et al., 2012; Francius and Clotman, 2014; Kabayiza et al., 2017), distribution (España and Clotman, 2012a,b; Audouard et al., 2013; Kabayiza et al., 2017), and maintenance (España and Clotman, 2012a,b; Stam et al., 2012) of specific neuronal populations, as well as the formation of

neuromuscular junctions (Audouard et al., 2012). Here, we demonstrate that OC factors regulate the diversification and the distribution of V2 INs during spinal cord development. Analyses of OC-deficient embryos showed defective production of specific subpopulations of V2a INs, as well as abnormal distribution of V2a and V2b cells in the developing spinal cord. Furthermore, we uncovered that OC proteins act upstream of specific spinal isoforms of *Pou2f2*, a POU family transcription factor. Using gain- or loss-of-function experiments, we demonstrated that, as observed for OC factors, *Pou2f2* regulates the distribution of V2 INs in the developing spinal cord. Thus, we uncovered a genetic pathway that regulates the diversification and the distribution of V2 INs during embryonic development.

RESULTS

OC Factors Are Present in Multiple Subsets of Spinal V2 INs

In the developing spinal cord, OC factors contribute to diversification, migration, and maintenance of different neuronal populations (Roy et al., 2012; Stam et al., 2012; Kabayiza et al., 2017). To study V2 IN diversification, we previously established a repertoire of markers that divide embryonic V2 cells into multiple subpopulations (Francius et al., 2013). Although OC factors have been detected in V2 INs (Francius and Clotman, 2010; Francius et al., 2013) and are similarly distributed at distinct antero-posterior levels (Francius et al., 2013), their production in V2 subsets has not been investigated yet. Therefore, we first determined the presence of each OC in these V2 subpopulations at e12.5.

V2a INs include neuronal subsets characterized by the presence of *Shox2*, *MafA*, *cMaf*, *Bhlhb5*, or *Prdm8* (Francius et al., 2013). Only *Hnf6* was detected in few *Shox2+* V2a cells (Figures 1A–C” and Table 1). In contrast, the three OC proteins were detected in *MafA+* and *cMaf+* V2a subpopulations (Figures 1D–I” and Table 1), but not in *Bhlhb5+* or *Prdm8+* cells (Table 1; data not shown). V2b INs include similar subsets except for *Shox2+* and *cMaf+* cells, and contain an additional *MafB+* subpopulation (Francius et al., 2013). OC were present in *MafA+* but not in *MafB+*, *Bhlhb5+*, or *Prdm8+* V2b subsets (Figures 1J–L” and Table 1; data not shown). In addition, OC were detected in V2c (non-progenitor *Sox1+* cells; Figures 1M–O” and Table 1) but not in V2d (*Shox2+Chx10-*) cells (Figures 1A–C” and Table 1). Thus, OC factors are present in multiple subpopulations of V2 INs.

OC Factors Regulate the Diversification of Spinal V2 INs

To determine whether OC proteins contribute to the development of V2 IN subsets, we characterized the phenotype of these cells in *Hnf6/Oc2* double-mutant embryos, which lack the three OC factors in the developing spinal cord (Roy et al., 2012; Kabayiza et al., 2017). Given that the number and the distribution of cells in each IN subpopulation vary along the anteroposterior axis of the spinal cord (Francius et al., 2013; Hayashi et al., 2018;

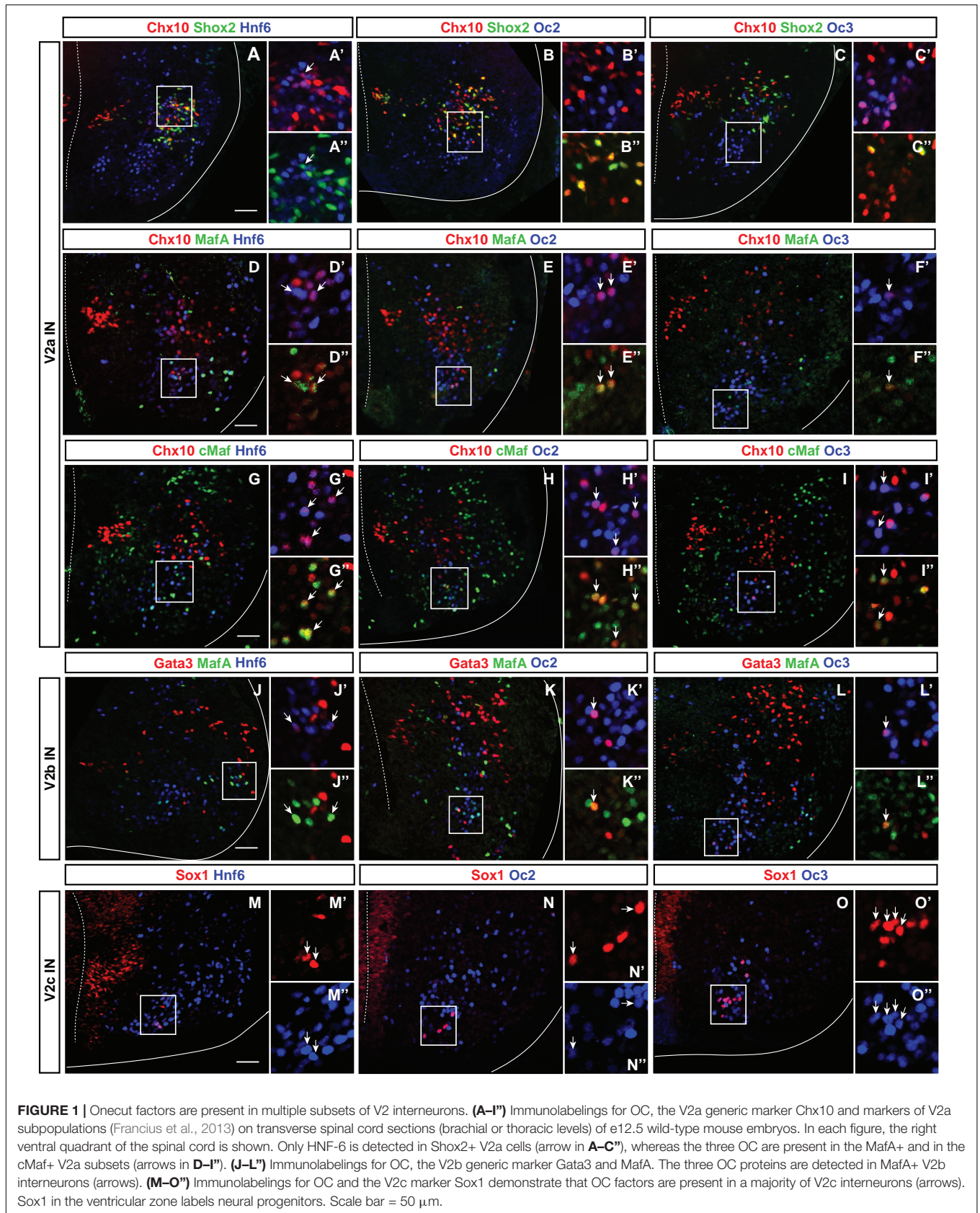


TABLE 1 | Onecut factors are present in specific populations and subpopulations of V2 interneurons.

		V2-e12.5		
Populations	Subpopulations	HNF-6	OC-2	OC-3
V2a-Chx10		+	+	+
	Shox2	+	–	–
	MafA	+	+	+
	cMaf	+	+	+
	Bhlhb5	–	–	–
	Prdm8	–	–	–
V2b-Gata3		+	+	+
	MafA	+	+	+
	MafB	–	–	–
	Prdm8	–	–	–
V2c-Sox1		+	+	+
V2d-Shox2		–	–	–

The V2 populations, including V2a, V2b, V2c, and V2d, are subdivided in smaller subpopulations characterized by differential expression of transcription factors (Francius et al., 2013). OC factors are detected in specific populations and subpopulations of V2 interneurons.

Sweeney et al., 2018), this analysis was systematically performed at brachial, thoracic and lumbar levels at e12.5 and e14.5.

In the absence of OC factors, the total number of Chx10+ INs was not significantly changed (Figures 2A–D and Supplementary Figures S1A,B), although a trend toward reduction was detected at brachial level at e12.5 (Figure 2C). Consistently, the number of Chx10+Shox2+ INs was not changed (Figures 2E–H and Supplementary Figures S1C–D”). These observations suggest that OC are not necessary for V2a IN production. In contrast, the smaller V2a subpopulations wherein OC factors were detected in control embryos, characterized by the presence of MafA (Figures 1D–F”) or cMaf (Figures 1G–I”), were almost completely lost in OC mutant embryos (Figures 2I–P and Supplementary Figures S1E–H”). As the total number of Chx10+ and of Shox2+ V2a was not changed (Figures 2A–H and Supplementary Figures S1A–D”), the loss of the MafA+ or cMaf+ subsets may be compensated for by expansion of other V2a subpopulations, markers of which remain to be identified. Nevertheless, our data indicate that OC factors are required either for the expression of V2 subpopulation markers or for the differentiation of specific V2a IN subsets.

To discriminate between these possibilities and to evaluate the contribution of OC factors to V2b diversification, we characterized the phenotype of V2b INs and of their MafA+ subpopulation in the absence of OC proteins. As observed for V2a INs, the total number of V2b cells was not changed in OC mutant embryos (Figures 2Q–T and Supplementary Figures S1I,J), although a trend toward reduction was observed at brachial level at e12.5 (Figure 2S). However, in contrast to V2a, the MafA+ V2b INs were present in normal number in OC mutant embryos (Figures 2U–X and Supplementary Figures S1K–L”). Hence, OC factors are not necessary for the production of the MafA+ V2b subset, although they are required

for proper differentiation of the MafA+ and of the cMaf+ V2a subpopulations.

Finally, we assessed the requirement for OC in the production of V2c INs, a V2 population strongly related to V2b cells (Panayi et al., 2010). Although weak production of Sox1 in spinal progenitors was preserved, V2c cells characterized by high Sox1 levels were scarcely detectable in OC mutant embryos at e12.5 (arrows in Figures 2Y–AA). However, the number of V2c was normal at e14.5 (Figure 2BB and Supplementary Figures S1M,N), suggesting that the absence of OC delays the differentiation of V2c INs without affecting the V2b population. Taken together, these observations demonstrate that OC proteins are not required for V2 IN production but regulate the diversification of V2 INs into multiple subpopulations.

OC Factors Regulate the Distribution of Spinal V2 INs

Although the total number of V2a or V2b INs was not affected by the absence of OC factors, careful examination of immunofluorescence labelings suggested that, as observed for spinal dorsal INs (Kabayiza et al., 2017), OC proteins may regulate the distribution of V2 INs in the developing spinal cord (Figures 2A,B,Q,R). Therefore, quantitative distribution analyses (Kabayiza et al., 2017) were performed for each V2 population at brachial, thoracic or lumbar levels at e12.5, namely in the course of ventral IN migration, and at e14.5, i.e., when ventral IN migration in the transverse plane of the spinal cord is completed. Absence of the MafA+ and cMaf+ V2a subpopulations in OC mutants and the small size of other V2 subsets prevented analysis of subpopulation distribution.

At e12.5 in control embryos, V2a INs distributed in two connected clusters, a major central group and a minor medial group, at each level of the spinal cord (Figures 3A–C). In mutant embryos, V2a cells similarly distributed in connected central and medial groups. However, the relative cell distribution between the two clusters was altered, with less central cells at brachial level and less medial cells at lumbar levels (Figures 3D–L). Altered V2a distribution on the medio-lateral axis was confirmed at e14.5. In control embryos, the two V2a groups did coalesce in a more evenly distributed population that occupied ~70% of the medio-lateral axis (Figures 3M–O). In mutant embryos, V2a INs remained segregated into two distinct, although connected, clusters with a majority of cells in medial position (Figures 3P–X). Thus, absence of OC factors perturbs proper distribution of the V2a INs and restricts at e14.5 migration of a fraction of V2a cells in a medial position.

To assess whether OC also regulate the position of other V2 populations, we studied the distribution of V2b INs. At e12.5 in control embryos, V2b cells distributed in a major central (brachial level) or lateral (thoracic and lumbar levels) cluster with minor subsets located more medially (arrows in Figures 4A–C) or ventrally (arrowheads in Figures 4A–C). In OC mutant embryos at e12.5, the major population was more compact, more centrally located and slightly more ventral. In addition, the ventral V2b subset was significantly depleted (Figures 4D–L). Consistently, at e14.5, V2b INs in the central

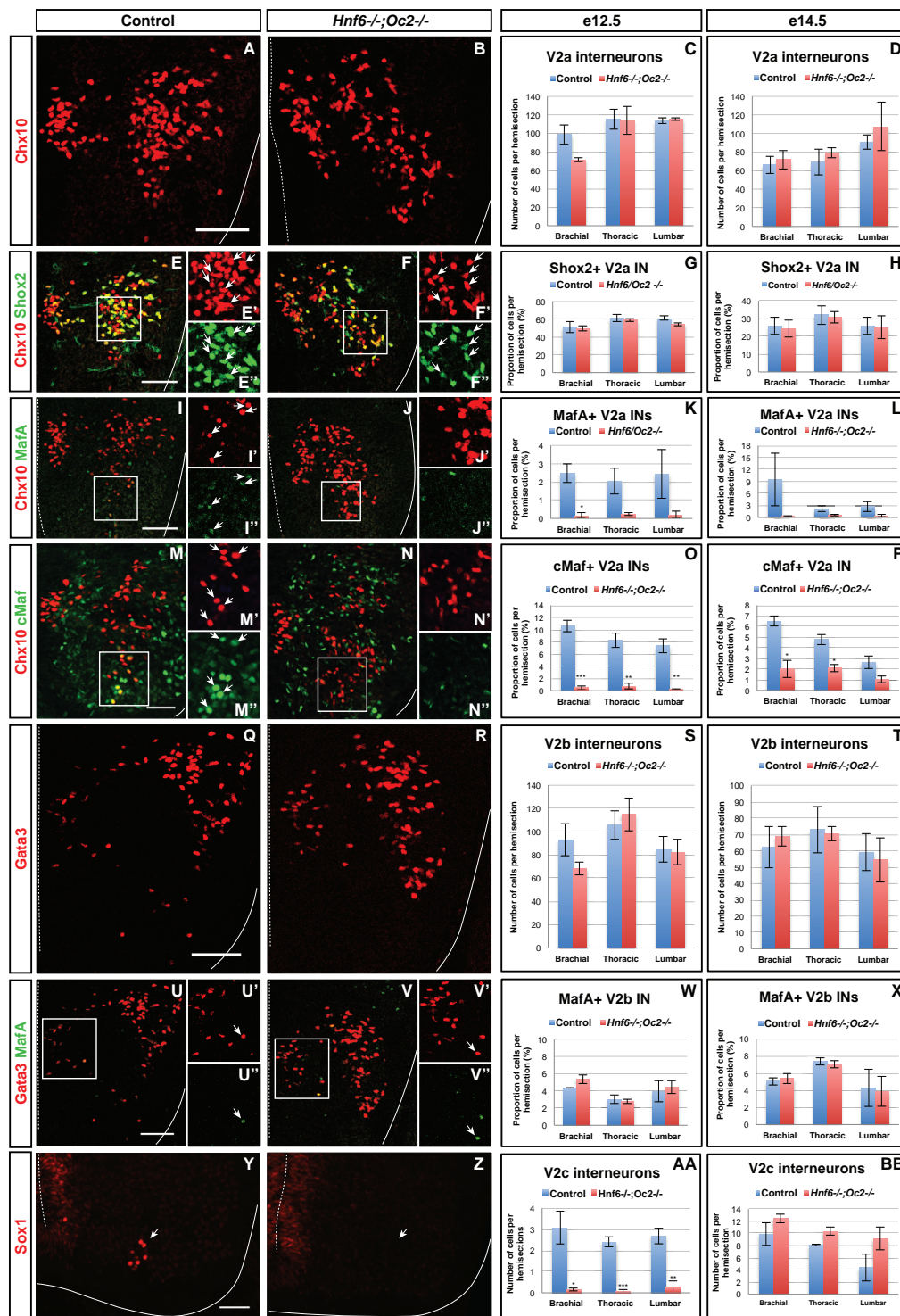


FIGURE 2 | Onecut factors regulate the diversification of the V2 interneurons. Immunolabelings on transverse spinal cord sections (brachial or thoracic levels) of control or *Hnf6*^{-/-};*Oc2*^{-/-} double-mutant embryos. At e12.5 (A–C) and e14.5 (D), the production of the V2a Chx10⁺ interneurons is not altered in the absence of OC factors. Similarly, the number of Shox2⁺ V2a is affected neither at e12.5 (E–G) nor at e14.5 (H). In contrast, quantitative analysis of control or *Hnf6*^{-/-};*Oc2*^{-/-} littermates at e12.5 (I–K) and at e14.5 (L) shows reduction in MafA⁺ V2a interneurons in double mutants as compared to control embryos. Similarly, the number of cMaf⁺ V2a interneurons is significantly reduced at e12.5 (M–O) and e14.5 (P) in the absence of OC factors. At e12.5 (Q–S) and e14.5 (T), the production of the V2b interneurons is not affected in *Hnf6*^{-/-};*Oc2*^{-/-} embryos. The generation of the MafA⁺ V2b interneurons is also unchanged at e12.5 (U–W) or e14.5 (X). At e12.5 (Y–AA), the number of V2c interneurons is dramatically reduced in the absence of OC factors (Sox1 in the ventricular zone labels neural progenitors). However, this is no longer the case at e14.5 (BB). Mean values ± SEM. **p* ≤ 0.05; ***p* ≤ 0.01; ****p* ≤ 0.001. Scale bar = 50 μm.

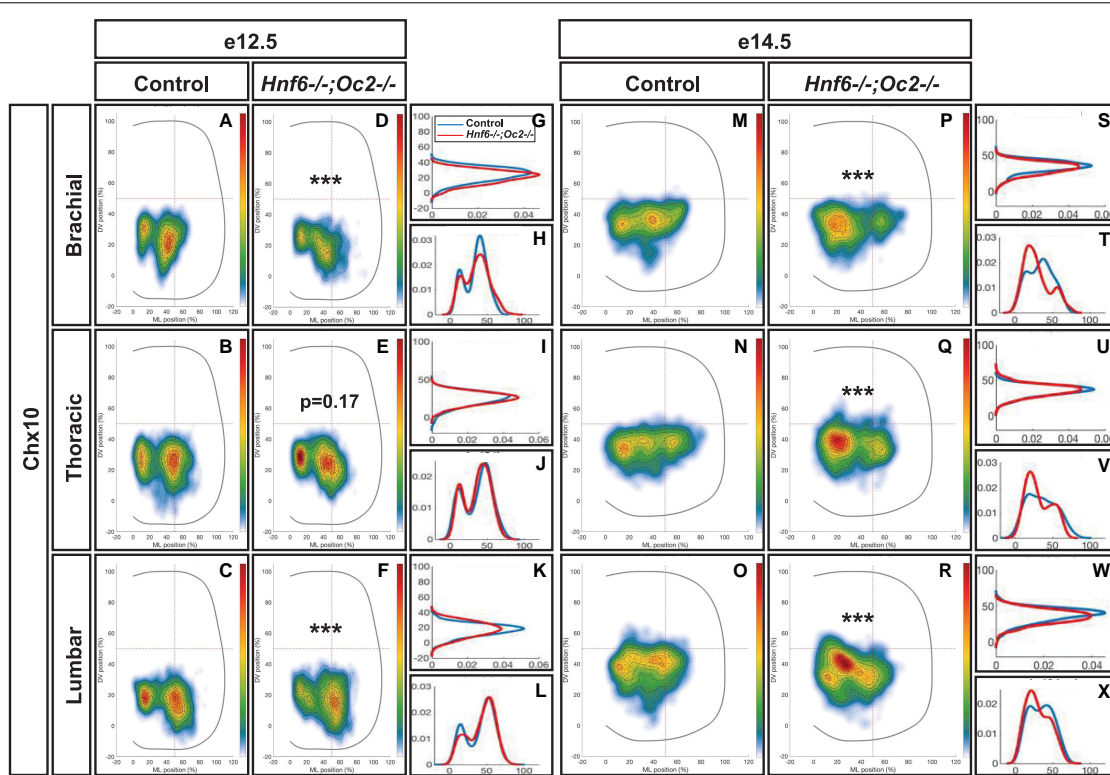


FIGURE 3 | One-cut factors regulate the distribution of V2a interneurons. Distribution of V2a interneurons on the transverse plane of the spinal cord in control or *Hnf6*^{-/-};*Oc2*^{-/-} double-mutant embryos at brachial, thoracic, or lumbar level (only the right hemisection is shown). Two-dimension distribution graphs (left) show integration of cell distribution from multiple sections of multiple embryos of each genotype. One-dimension graphs (right) compare density distribution in control (blue) and in double-mutant embryos (red) on the dorso-ventral (upper) or the medio-lateral (lower) axis of the spinal cord (see section “Materials and Methods” for details). **(A–C)** At e12.5 in control embryos, V2a interneurons distribute in two connected clusters, a major central group and a minor medial group, at each level of the spinal cord. **(D–L)** In mutant embryos, the relative cell distribution between the two clusters seems altered, with relatively less central cells at brachial level and less medial cells at lumbar levels ($n = 3$, $p \leq 0.001$ at brachial and lumbar levels; $p = 0.17$ at thoracic level). **(M–X)** Altered V2a distribution on the medio-lateral axis is confirmed at e14.5. **(M–O, S–X)** In control embryos, the two V2a groups coalesce in a more evenly distributed population that occupied ~70% of the medio-lateral axis. **(P–X)** In mutant embryos, V2a interneurons remain segregated into two distinct, although connected, clusters with a majority of cells in medial position ($n = 3$, $p \leq 0.001$).

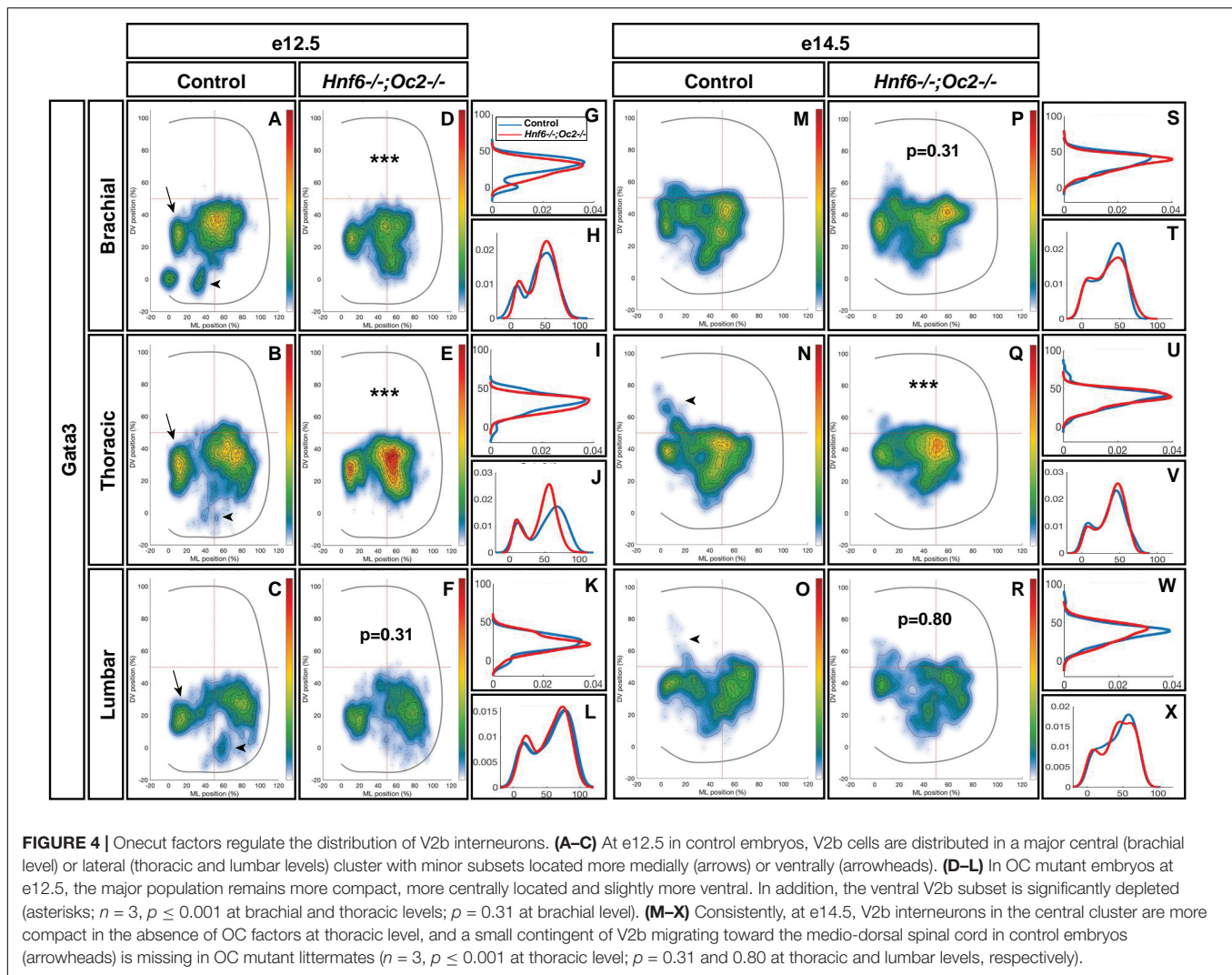
cluster remained significantly more compact at thoracic level in the absence of OC factors, and identical trends were observed at brachial and lumbar levels (Figures 4M–X). In addition, a small contingent of V2b migrating toward the medio-dorsal spinal cord in control embryos (arrowheads in Figures 4N,O) was missing in OC mutant littermates (Figures 4Q–X). Taken together, these observations demonstrate that, in addition to V2 diversification, the OC transcription factors regulate proper distribution of V2 INs during spinal cord development.

OC Factors Control Expression of Neuronal-Specific Isoforms of *Pou2f2*

To identify genes downstream of OC that may contribute to V2 IN differentiation and distribution, we performed a microarray comparison of control and of OC-deficient spinal cord transcriptome at e11.5, namely at the stage when significant numbers of V2 cells have been generated and are initiating migration (GEO repository accession number: GSE117871). Among genes showing a differential expression level in the OC mutant spinal cord (Supplementary Table S1), *Pou2f2* was significantly upregulated (1.57-fold increase). *Pou2f2* (previously

named Oct-2) is a transcription factor containing a POU-specific domain and a POU-type homeodomain (Figure 5A) that binds an octamer motif (consensus sequence ATGCAAAT) (Latchman, 1996). *Pou2f2* expression has been detected in B lymphocytes, in neuronal cell lines and in neural tissues including the developing CNS (Hatzopoulos et al., 1990; Lillycrop and Latchman, 1992; Camos et al., 2014). *Pou2f2* is required for differentiation of B lymphocytes and for postnatal survival (Corcoran et al., 1993; König et al., 1995; Corcoran et al., 2004; Hodson et al., 2016), and is able to modulate neuronal differentiation of ES cells (Theodorou et al., 2009). However, its role in the developing spinal cord remains unknown.

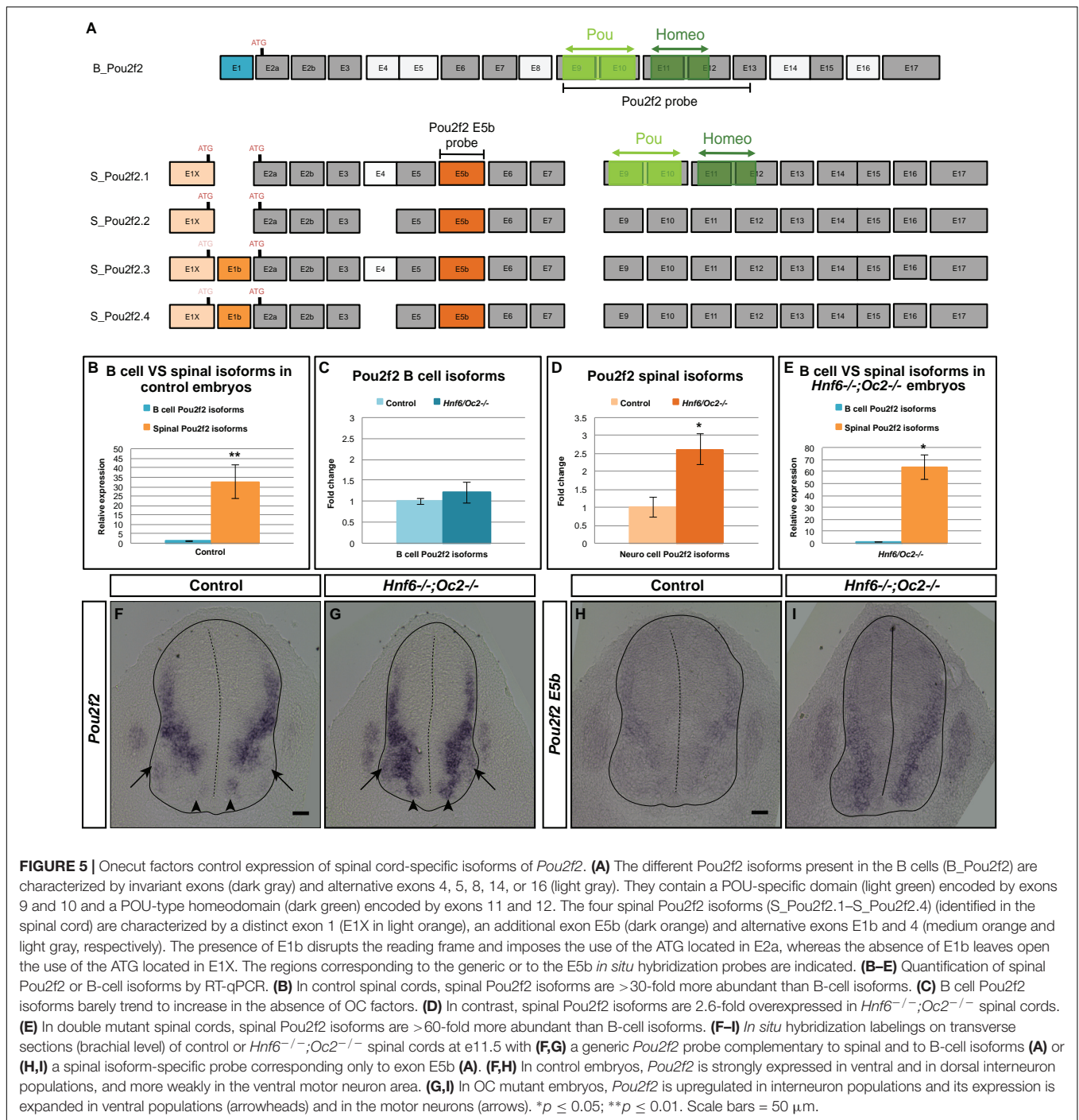
Based on work in B cells, multiple *Pou2f2* isoforms generated by alternative splicing have been described (Figure 5A; Hatzopoulos et al., 1990; Wirth et al., 1991; Lillycrop and Latchman, 1992; Stoykova et al., 1992; Liu et al., 1995). Therefore, we first determined whether similar isoforms are found in the developing spinal cord. However, we systematically failed to obtain RT-PCR products using upstream primers in described exon 1 (asterisks in Supplementary Figures S2A,B and data not shown; Table 2) and amplifications encompassing exons 5 to 6 generated predominant amplicons larger than



expected (arrowheads in **Supplementary Figure S2B** and **Table 2**), suggesting the existence of alternative exons in *Pou2f2* embryonic spinal cord transcripts (**Figure 5A**). Data mining the NCBI Nucleotide database for *Pou2f2* sequences identified a predicted murine *Pou2f2* isoform (X6 sequence, accession number XM_006539651.3) with a different exon 1 (E1X) and an additional sequence between exons 5 and 6, the size of which (279 bp) corresponded to the size differences estimated in our amplifications encompassing exons 5 to 6 (arrowheads in **Supplementary Figure S2B** and **Table 2**). Using PCR primers in this predicted sequence, we were able to amplify a 5' region of *Pou2f2* from the alternative E1X exon and an additional sequence between exons 5 and 6 (**Supplementary Figure S2C** and **Table 2**), suggesting that alternative isoforms similar to this predicted sequence are produced in the developing spinal cord. However, amplifications from E1X systematically produced two amplicons (arrowheads in **Supplementary Figure S2C** and **Table 2**), suggesting the existence of an alternative exon downstream to E1X. Sequencing of our PCR products and alignment to genomic DNA confirmed that predominant *Pou2f2*

isoforms in the developing spinal cord contain the alternative E1X exon, an additional exon (E5b) between exons 5 and 6, and can undergo alternative splicing of a short (61bp) exon (E1b) between E1X and exon 2 (**Supplementary Figure S2D**). E5b exon maintains the reading frame. In contrast E1b exon disrupts it, imposing the use of the ATG located in exon 2 to generate a functional *Pou2f2* protein, whereas the absence of E1b leaves open the use of an alternative upstream ATG located at the 3' end of E1X (**Figure 5A** and **Supplementary Figure S2D**). Hence, our RT-PCR and sequencing data indicate that four neuronal *Pou2f2* isoforms different from the previously described B-cell or neural isoforms are produced in the developing spinal cord (**Figure 5A**).

However, minor transcripts corresponding to B-cell isoforms are also detected in the embryonic spinal cord (**Supplementary Figures S2A,B** and **Table 2**). To assess the relative abundance of each transcript type in this tissue and to evaluate the extent of their relative overexpression in the absence of OC factors, we quantified each isoform type in control and in OC-deficient spinal cord at e11.5. In control spinal cords, spinal *Pou2f2* isoforms were >30-fold more abundant than B-cell



isoforms (Figure 5B), consistent with our RT-PCR observations (Supplementary Figure S2). In the absence of OC factors, spinal isoforms were ~2.6-fold overexpressed whereas B-cell isoforms barely trended to increase (Figures 5C–E). Thus, OC factors repress expression of spinal *Pou2f2* isoforms in the developing spinal cord.

To confirm these data and to determine the expression pattern of *Pou2f2* in the ventral spinal cord, *in situ* hybridization was performed on sections from control or *Hnf6*/*Oc2* double-mutant

spinal cords using either a generic *Pou2f2* probe complementary to spinal and to B-cell isoforms or a spinal isoform-specific probe corresponding only to exon E5b (Figure 5A). Using the generic *Pou2f2* probe on control tissue, we detected *Pou2f2* transcripts in the ventral region of the spinal cord, with lower expression levels in the location of the motor columns (arrows in Figure 5F). In OC mutant embryos, *Pou2f2* expression was globally increased and additionally expanded in the ventral area (arrowheads in Figures 5E,G) including the motor neuron territories (arrows in

TABLE 2 | Pou2f2 isoforms in the developing spinal cord are different from B-cell isoforms.

Amplification	Expected sizes	B cells	Control spinal cord
E1 → E6	272 bp	272 bp	No amplification ^a
	390 bp	390 bp	
	456 bp	456 bp	
E7 → E9	174 bp	174 bp	174 bp
	222 bp	222 bp	
E10 → E12	452 bp	452 bp	452 bp
	160 bp	160 bp	
E13 → E17	296 bp	296 bp	370 bp
	370 bp	370 bp	
E1 → E7	348bp	466 bp	No amplification ^a
	466 bp	532 bp	
	532 bp		
E2 → E7	284 bp	402 bp	~680 bp ^a
	402 bp	468 bp	~750 bp ^a
	468 bp		
E3 → E6			272 bp ^a
	154 bp	154 bp	378 bp ^a
	272 bp	272 bp	~550 bp ^a
	378 bp	378 bp	~650 bp ^a
E4 → E7	340 bp	340 bp	~600 bp ^a
			201 bp ^a
E5 → E7	201 bp	201 bp	~480 bp ^a
			160 bp
E6 → E7	160 bp	160 bp	160 bp
			152 bp ^a
E1X → E3	152 bp	No amplification ^a	~220 bp ^a
E1X → E5b	554 bp	N.D	554 bp
	620 bp		620 bp
E5b	234 bp	N.D	234 bp
E3 → E5b	429 bp	N.D	429 bp
	495 bp		495 bp
E5b → E7	416 bp	N.D	416 bp

Regions covering B lymphocytes or predicted Pou2f2 isoforms (exons E1 or E1X to E17) were amplified by RT-PCR from lymphocyte or embryonic spinal cord RNA. ^aUnexpected results.

Figures 5F,G). Similar observations were made with the spinal isoform-specific probe (**Figures 5H,I**). Thus, OC factors restrict and moderate *Pou2f2* expression in ventral spinal populations likely including V2 INs.

Pou2f2-Positive V2 INs Are Mislocated in the Absence of OC Factors

To assess whether increased *Pou2f2* expression in *Hnf6^{-/-};Oc2^{-/-}* spinal cords corresponded to an expansion of *Pou2f2* distribution in V2 INs or an upregulation in its endogenous expression territory, we first quantified the number and distribution of *Pou2f2*-containing Chx10+ cells at e12.5 and e14.5 (**Figure 6** and **Supplementary Figure S3**). Immunofluorescence experiments demonstrated that *Pou2f2* is present in V2a INs in control embryos (**Figures 6A,C** and **Supplementary Figures S3A,D**), although it was only sparsely detected in MafA+ and cMaf+ V2a subsets (data not shown). Intensity of the labeling confirmed increased *Pou2f2* production in the ventral regions of the spinal cord in

OC mutant embryos (**Figures 6A–F**). However, the number in *Pou2f2*-positive V2a INs was not significantly different (**Figures 6E,F** and **Supplementary Figure S3**), suggesting that *Pou2f2* is increased in its endogenous expression domain. In contrast, the distribution of *Pou2f2*-positive V2a INs was affected (**Figures 6A–D,G–DD**). At e12.5, cells in the central clusters were slightly reduced at brachial and at thoracic levels (**Figures 6G–R**). In contrast, at e14.5, a majority of V2a containing *Pou2f2* settled in a medial position (**Figures 6S–DD**), reminiscent of the distribution defects observed for the whole V2a population (**Figure 3**). Similarly, *Pou2f2* was detected in V2b INs in control embryos, although in a more restricted number of cells (**Figures 7A,B,E**). In the absence of OC factors, the number of *Pou2f2*-positive V2b cells was not significantly increased (**Figures 7C,D,F**) but, as observed for V2a, this subset of V2b INs was mislocated with cells more central at e12.5 and more clustered on the medio-lateral axis at e14.5 (**Figures 7G–DD**). Taken together, these observations suggest that *Pou2f2* may contribute to control V2 IN migration during spinal cord development and could participate in alterations of V2 distribution in the absence of OC factors.

Pou2f2 Regulates the Distribution of Spinal V2 INs

To determine whether *Pou2f2* is able to modulate V2 IN distribution, we mimicked increased expression of this transcription factor observed in OC mutant embryos by overexpressing *Pou2f2* in the chicken embryonic spinal cord (**Supplementary Figure S4**). Increased *Pou2f2* did not impact on the number of V2a or V2b (**Figures 8A–F**). In contrast, it did alter V2 IN location. In HH27-28 control spinal cord, V2a INs were distributed in two closely connected clusters on the medio-lateral axis of the neuroepithelium (**Figure 8G**). In electroporated spinal cord, lateral migration was increased and a majority of V2a INs were clustered in a single group in a central position (**Figures 8H–J**) with ectopic lateral extensions (arrow in **Figure 8H**). In control spinal cord, V2b were distributed in two groups along the medio-lateral axis with a majority of cells in the lateral cluster (**Figure 8K**). In electroporated spinal cord, the V2b INs were equally distributed between these two clusters (**Figures 8L–N**). Thus, consistent with our observation in OC mutant embryos, increased *Pou2f2* can modulate the distribution of V2 INs in the developing spinal cord.

To confirm the influence of *Pou2f2* on V2 migration, we studied V2 distribution in mouse embryos devoid of *Pou2f2* (Corcoran et al., 1993) at e12.5. Absence of *Pou2f2* did not impact on the number of V2a INs (**Figures 9A–C**) nor on the Shox2+, cMaf+, or MafA+ V2a subsets (**Supplementary Figure S5**). In contrast, V2a distribution was affected in *Pou2f2* mutants. As compared to the two V2a clusters observed in control embryos, Chx10+ cells were more scattered in *Pou2f2* mutant embryos (**Figures 9D–O**). Furthermore, although the number of V2b, V2c, or MafA+ V2b cells was not changed in the absence of *Pou2f2* (**Figures 10A–C** and **Supplementary Figure S6**), V2b cells remained more medial at brachial and thoracic levels and segregated more extensively on the medio-lateral axis at lumbar

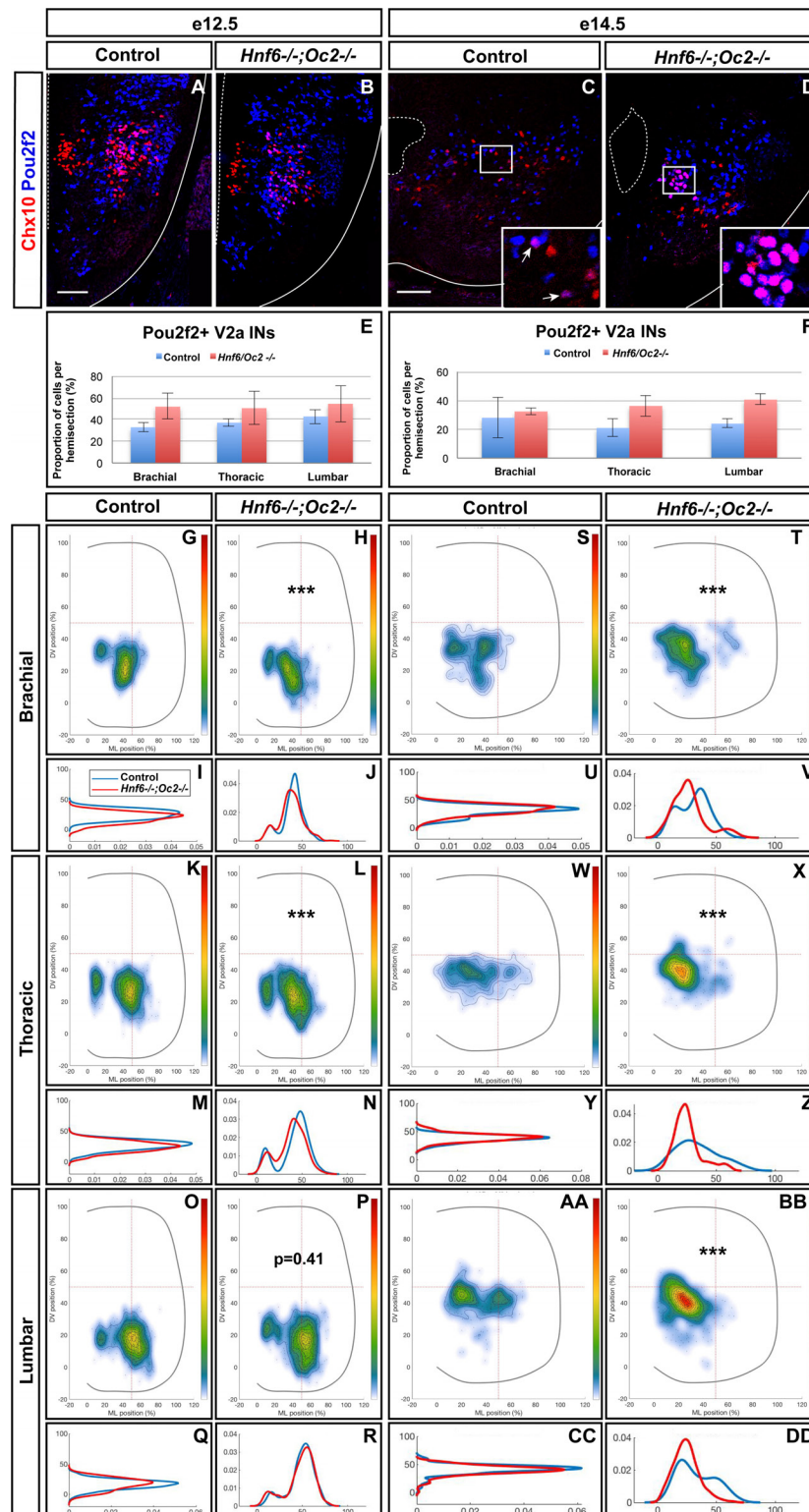


FIGURE 6 | The Pou2f2+ V2a interneurons are mislocated in the absence of OC factors. **(A–F)** Immunolabelings and quantification of Pou2f2+ V2a interneurons in control or *Hnf6*^{-/-};*Oc2*^{-/-} mutant embryos. At e12.5 **(A,B)** and e14.5 **(C,D)**, Pou2f2 is detected in V2a Chx10⁺ interneurons, and the number of Pou2f2-containing Chx10⁺ cells tends to increase but is not significantly different in the absence of OC factors **(E,F)**. **(G–DD)** Distribution of Pou2f2+ V2a interneurons on the transverse plane of the spinal cord in control or *Hnf6*^{-/-};*Oc2*^{-/-} double-mutant embryos. One-dimension graphs (lower) show density distribution on the dorso-ventral (left) or the medio-lateral (right) axis of the spinal cord. **(G–R)** At e12.5, cells in the central clusters are slightly reduced at brachial and at thoracic levels in the absence of OC factors ($n = 3$, $p \leq 0.001$ at brachial and thoracic levels; $p = 0.41$ at lumbar level). **(S–DD)** At e14.5, a vast majority of V2a containing Pou2f2 settles in a more medial position in *Hnf6*^{-/-};*Oc2*^{-/-} spinal cords ($n = 3$, $p \leq 0.001$). Mean values \pm SEM. Scale bar = 50 μ m.

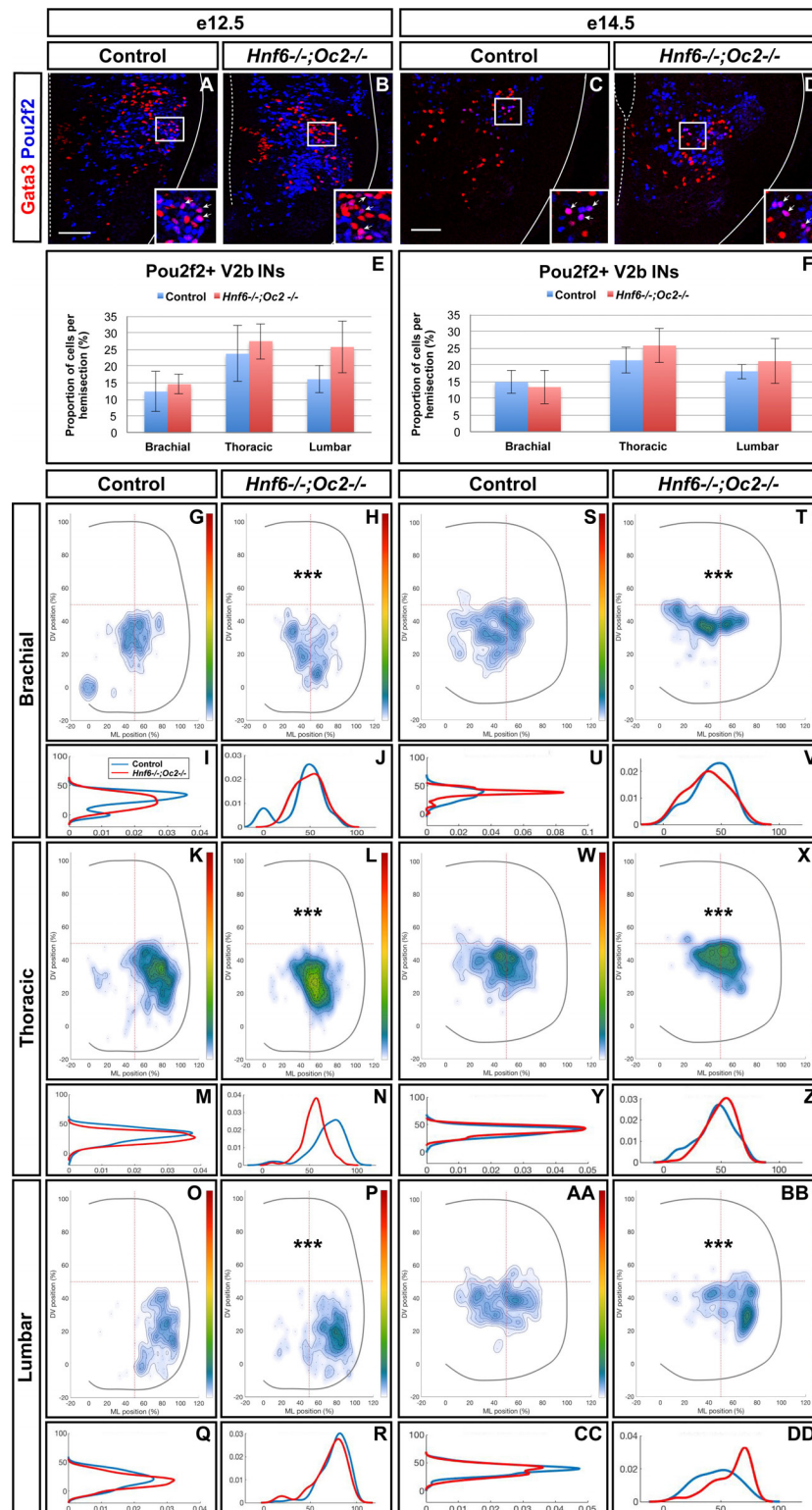
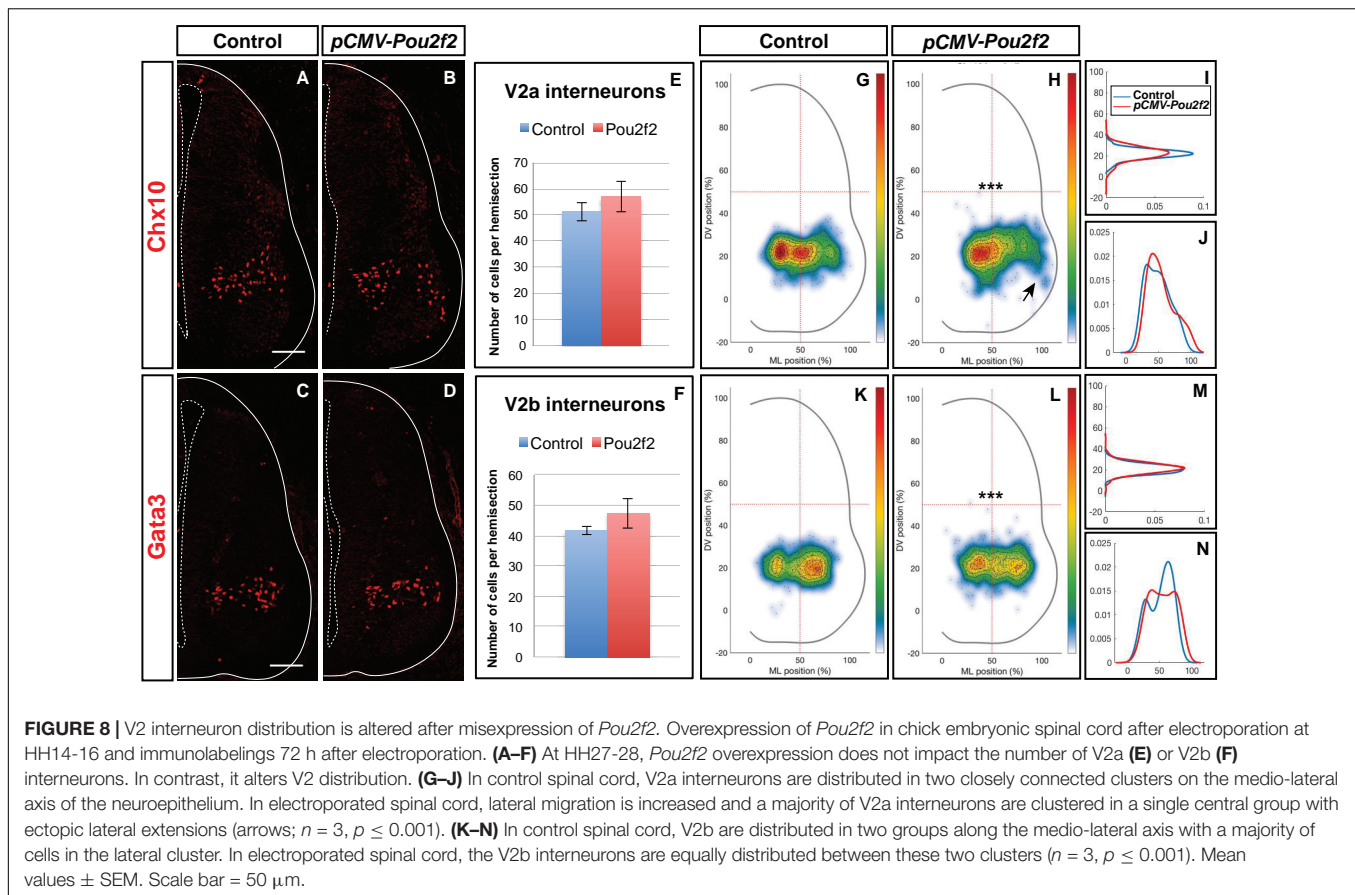


FIGURE 7 | The Pou2f2+ V2b interneurons are mislocated in the absence of OC factors. **(A–F)** Immunolabelings and quantification of Pou2f2+ V2b interneurons in control or *Hnf6*^{-/-};*Oc2*^{-/-} mutant embryos. At e12.5 **(A,B)** and e14.5 **(C,D)**, Pou2f2 is present in V2b Gata3+ interneurons, but the number of Pou2f2+ V2b cells was not significantly increased in the absence of OC factors **(E,F)**. **(G–DD)** Distribution of Pou2f2+ V2b interneurons on the transverse plane of the spinal cord in control or *Hnf6*^{-/-};*Oc2*^{-/-} double-mutant embryos. One-dimension graphs (lower) show density distribution on the dorso-ventral (left) or the medio-lateral (right) axis of the spinal cord. **(G–R)** At e12.5, Pou2f2-containing V2b are more central and slightly more ventral in the absence of OC factors ($n = 3$, $p \leq 0.001$). **(S–DD)** At e14.5, this subset of V2b interneurons is more clustered on the medio-lateral axis in *Hnf6*^{-/-};*Oc2*^{-/-} spinal cords ($n = 3$, $p \leq 0.001$). Mean values \pm SEM. Scale bar = 50 μ m.



levels (Figures 10D–O). Taken together, these observations demonstrate that *Pou2f2* regulate the distribution of V2 INs during spinal cord development.

DISCUSSION

In the recent years, several studies demonstrated that proper distribution of neuronal populations and subpopulations in the developing spinal cord is critical for adequate formation of spinal circuits (Surmeli et al., 2011; Tripodi et al., 2011; Goetz et al., 2015; Bikoff et al., 2016; Hilde et al., 2016; Hayashi et al., 2018). However, the genetic programs that control the diversification of spinal neuronal populations into specialized subpopulations and the proper settling of these neuronal subsets in the spinal parenchyma remain elusive. Here, we provide evidence that OC transcription factors regulate the diversification of spinal V2 INs, and that a genetic cascade involving OC factors and their downstream target *Pou2f2* controls the distribution of V2 INs in the developing spinal cord.

Control of V2 IN Diversification by the OC Factors

Cardinal populations of spinal ventral INs have been well characterized, and their global contribution to the activity of motor circuits has been extensively studied (reviewed in

(Gosgnach et al., 2017; Ziskind-Conhaim and Hochman, 2017; Boije and Kullander, 2018). However, more recently, the idea emerged that these cardinal populations are not homogeneous ensembles but rather contain multiple neuronal subsets with distinct molecular identities and functional properties (Borowska et al., 2013; Francius et al., 2013; Talpalar et al., 2013; Borowska et al., 2015; Bikoff et al., 2016; Sweeney et al., 2018). V2a INs comprise two major divisions, namely type I and type II V2a cells, that are arrayed in counter-gradients along the antero-posterior axis of the spinal cord and activate different patterns of motor output at brachial or lumbar levels. Furthermore, these two large divisions can themselves be fractionated at birth into 11 subsets characterized by distinct combinations of markers, differential segmental localization and specific distribution patterns on the medio-lateral axis of the spinal cord (Hayashi et al., 2018). In the zebrafish, three distinct subclasses of V2a INs participate in separate microcircuit modules driving slow, intermediate or fast motor neuron activity (Ampatzis et al., 2014). Taken together, these observations suggest that cardinal IN populations only constitute the first organization level of functionally distinct neuronal subsets that contribute to diversity and flexibility within spinal motor circuits.

We showed here that OC factors are present in subsets of V2 INs and contribute to their diversification. Normal numbers of cardinal V2a and V2b cells were generated in OC mutant embryos, suggesting that these factors do not contribute to the

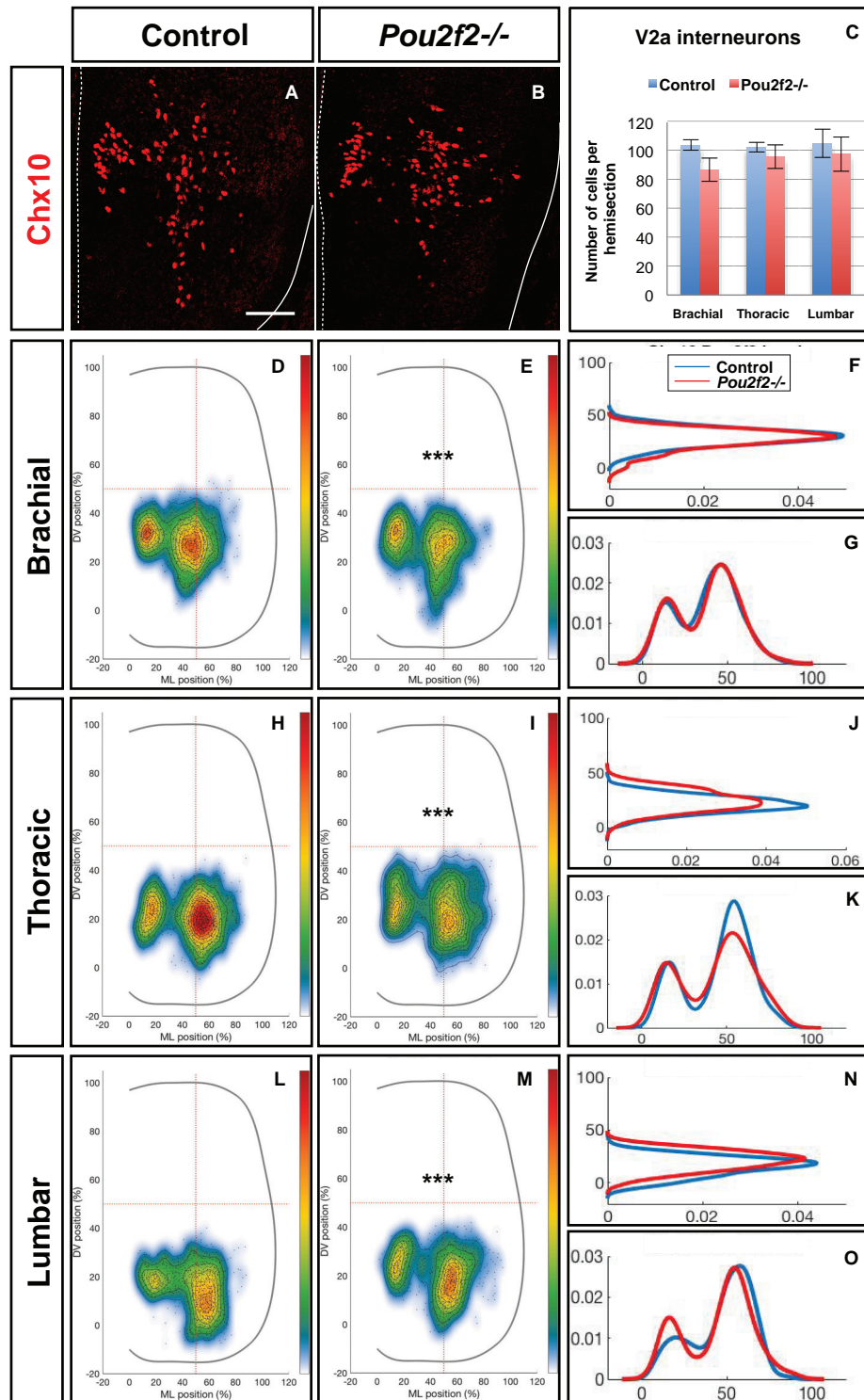


FIGURE 9 | *Pou2f2* regulate the distribution of V2a interneurons. (A–C) Immunolabelings and quantification of V2a interneurons in control or *Pou2f2*^{-/-} mutant embryos. At e12.5, the production of the Chx10+ V2a interneurons is not altered in absence of *Pou2f2*. (D–O) Distribution of V2a and Shox2+ V2a interneurons on the transverse plane of the spinal cord in control or *Pou2f2*^{-/-} mutant embryos. One-dimension graphs (right) show density distribution on the dorso-ventral (upper) or the medio-lateral (lower) axis of the spinal cord. V2a distribution is affected in *Pou2f2*^{-/-} mutants. As compared to the two V2a clusters observed in control embryos, Chx10+ cells are relatively more abundant in the medial cluster in *Pou2f2*^{-/-} mutant embryos ($n = 3$, $p \leq 0.001$). Mean values \pm SEM. Scale bar = 50 μ m.

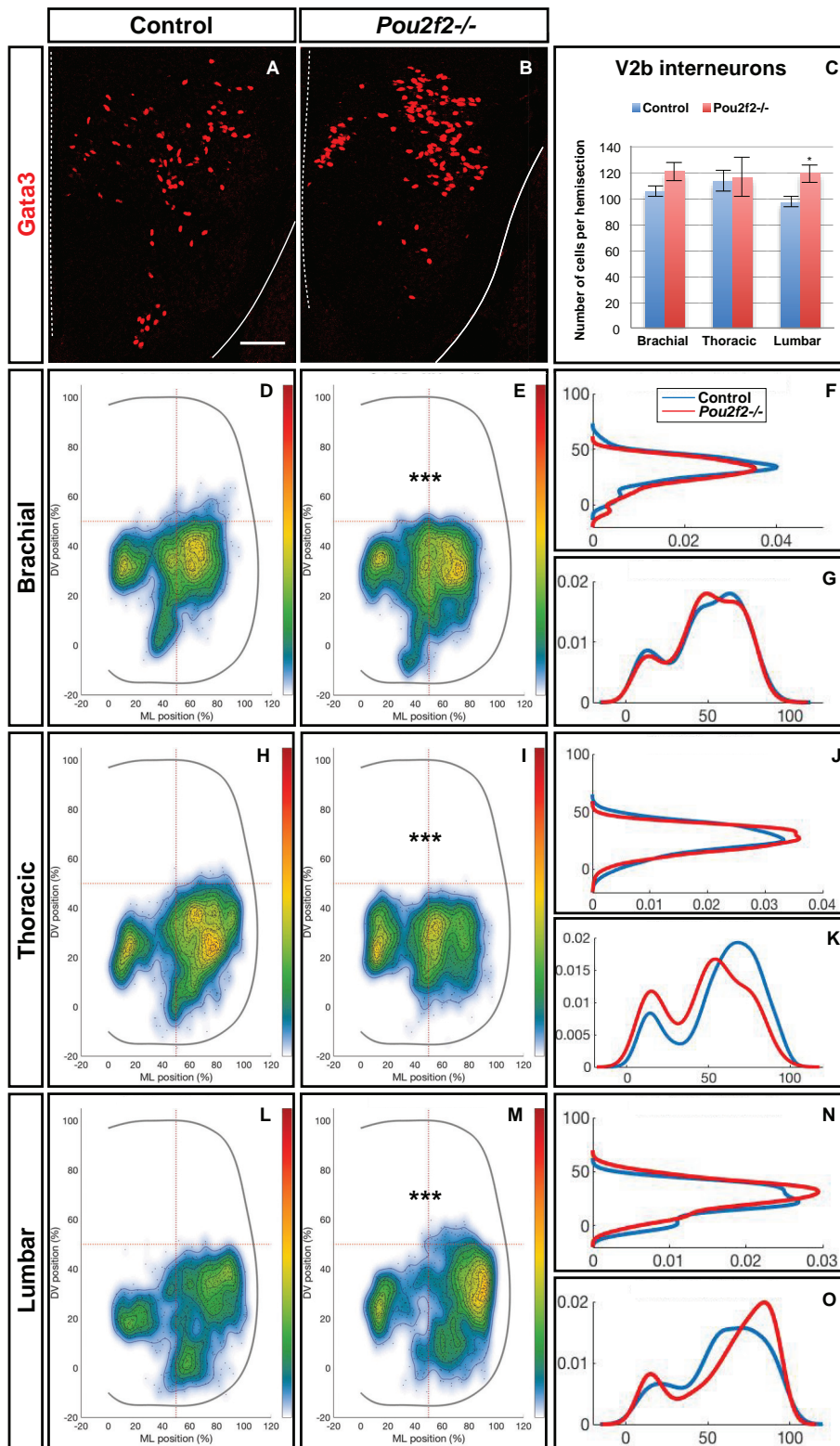


FIGURE 10 | *Pou2f2* regulate the distribution of V2b interneurons. **(A–C)** Immunolabelings and quantification of V2b interneurons in control or *Pou2f2*^{-/-} mutant embryos. At e12.5, the production of the Gata3+ V2b interneurons is not affected by the absence of *Pou2f2*. **(D–O)** Distribution of V2b interneurons on the transverse plane of the spinal cord in control or *Pou2f2*^{-/-} mutant embryos. One-dimension graphs (right) show density distribution on the dorso-ventral (upper) or the medio-lateral (lower) axis of the spinal cord. The distribution of V2b cells is altered in *Pou2f2*^{-/-} mutants, as V2b interneurons remained more medial at thoracic level and segregated more extensively on the medio-lateral axis at lumbar level ($n = 3, p \leq 0.001$). Mean values \pm SEM. Scale bar = 50 μ m.

production of V2 cells (Thaler et al., 2002; Lee et al., 2008; Clovis et al., 2016) nor to the segregation of the V2a and V2b lineages through differential activation of Notch signaling (Del Barrio et al., 2007; Peng et al., 2007; Joshi et al., 2009; Misra et al., 2014). In contrast, V2a subpopulations characterized by the presence of MafA or cMaf were strongly depleted in the absence of OC proteins. This observation results either from a loss of these V2a subsets or from a downregulation of *MafA* or *cMaf* expression in these cells. Incomplete knowledge of the whole collection of V2a subsets prevented to assess whether this apparent loss of specific subpopulations was compensated for by an expansion of neighboring subsets. Nevertheless, these data demonstrate altered differentiation of V2 IN subsets in the absence of OC factors, as previously observed for spinal motor neurons (Roy et al., 2012) and dorsal INs (Kabayiza et al., 2017). In addition, the production of V2c cells was delayed in OC mutant embryos, although V2b that are supposed to constitute the source of V2c (Panayi et al., 2010) were timely generated. This points to a specific contribution of OC protein to the development of V2c INs, the mechanism of which is currently unknown.

Control of V2 IN Distribution by the OC Factors

Beside diversification, the characterization of functionally distinct IN subpopulations unveiled a strong correlation between the distribution of each IN subset and their contribution to distinct microcircuit modules (Tripodi et al., 2011; Borowska et al., 2013; Goetz et al., 2015; Bikoff et al., 2016; Hilde et al., 2016; Hayashi et al., 2018). These data support a model wherein correct localization of spinal IN subsets is critical for proper formation of sensory and sensory-motor circuits, highlighting the importance of a strict regulation of short-distance neuronal migration in the developing spinal cord. However, genetic determinants that control spinal IN migration have only been sparsely identified. *Sim1* regulate ventro-dorsal migration of the V3 IN subsets (Blacklaws et al., 2015). Similarly, *SATB2* control the position of inhibitory sensory relay INs along the medio-lateral axis of the spinal cord (Hilde et al., 2016). Here, we provide evidence that the OC factors control a genetic program that regulates proper positioning of V2 INs during embryonic development. In the absence of OC proteins, a fraction of V2a INs remained in a more medial location, expanding the medial cluster containing locally projecting cells at the expense of the lateral cluster that comprises the supraspinal-projecting V2a INs (Hayashi et al., 2018). V2b alterations were less spectacular, although ventral and dorsal contingents were reduced and the cell distribution in the central cluster was altered. Variability in the alterations observed at e12.5 and e14.5 highlights that spinal migration is not completed at e12.5 and suggests that distribution of earlier- or later-migrating neurons may be differently affected by the absence of OC proteins. In addition, migration along the anteroposterior axis, which can not be analyzed in our experimental setup, could also be perturbed. Alterations of the distribution of V2a and V2b interneurons likely correlate with alterations in their differentiation program. Indeed, the

production of adequate clues to ensure proper cell positioning is an intrinsic component of any neuronal differentiation program (Blacklaws et al., 2015; Hilde et al., 2016; Hayashi et al., 2018). In any case, our observations are consistent with the contribution of OC factors to the migration of several populations of spinal dorsal INs (Kabayiza et al., 2017). This raises the question whether similar cues might be regulated by identical genetic programs and used by different IN populations to organize proper distribution of ventral and dorsal IN subsets in the developing spinal cord. Identification of the factors downstream of OC protein involved in the control of neuronal migration will be necessary to answer this question.

An OC-Pou2f2 Genetic Cascade Regulates the Migration of V2 INs

Therefore, we attempted to identify genes downstream of OC factors and possibly involved in the control of IN migration using a global approach comparing the transcriptome of whole spinal cords isolated from control or OC-deficient embryos. Absence of known regulators of neuronal migration among the most affected genes suggests that different actors may be active downstream of OC proteins in distinct IN populations to regulate proper neuronal distribution. In contrast, we uncovered that expression of the transcription factor *Pou2f2* is repressed by OC factors in different spinal populations. Surprisingly, our data demonstrated that variant *Pou2f2* isoforms are produced in the developing spinal cord as compared to B lymphocytes (Hatzopoulos et al., 1990; Wirth et al., 1991; Lillycrop and Latchman, 1992; Stoykova et al., 1992; Liu et al., 1995), and that these spinal variants are regulated by OC proteins. Spinal-enriched transcripts encode *Pou2f2* proteins containing additional peptidic sequences upstream of the POU-specific domain and of the homeodomain. Furthermore, exon 1 is different and corresponds to sequences located ~47kb upstream of the transcription initiation site used in B cells (data not shown) in the mouse genome, suggesting that OC regulate *Pou2f2* expression from an alternative promoter. However, we cannot exclude that additional exon(s) could be present upstream of the identified sequences, and determination of the regulating sequences targeted by the OC protein will require thorough characterization of the produced transcripts. In addition, we cannot rule out indirect regulation of *Pou2f2* expression by the OC factors, as OC are usually considered to be transcriptional activators rather than repressors (Jacquemin et al., 2000; Lannoy et al., 2000; Jacquemin et al., 2003a; Pierreux et al., 2004; Beaudry et al., 2006; Roy et al., 2012).

Nevertheless, our observations demonstrate that *Pou2f2* is downstream of OC factors in the V2 INs and also contributes to regulate the distribution of V2 INs during embryonic development. The number of *Pou2f2*-containing V2 was not significantly increased in OC mutant spinal cords, suggesting that the absence of OC protein resulted in relaxing of *Pou2f2* production in its endogenous expression domain rather than ectopic activation in other V2 subsets. Increased production of *Pou2f2* in the chicken embryonic

spinal cord resulted in alterations in the localization of V2 populations without any change in cell number, pointing to a possible contribution of *Pou2f2* to the regulation of V2 migration downstream of OC factors. However, spinal cord electroporation experiments are constrained by the developmental stage selected to target ventral INs and by the duration of the incubation to maintain viable embryos, which does not enable to compare IN migration in mouse and chicken at later developmental stages. These also limited chicken loss-of-function studies, which would additionally be hampered by incomplete inhibition of gene expression. Nevertheless, our observations suggested that *Pou2f2* may regulate V2 IN migration.

Consistently, V2 distribution was perturbed in *Pou2f2* mutant embryos without any alteration in V2 population or subpopulation cell numbers, demonstrating the involvement of *Pou2f2* in the control of V2 IN distribution. Alterations in V2 distribution after *Pou2f2* electroporation were not comparable to that observed in OC mutant embryos and were not strictly opposite to *Pou2f2* knockout phenotype because the developmental stages obtained after chicken embryo electroporation were much earlier than the developmental stages of analyzed mouse embryos. Nevertheless, our data demonstrate that a genetic cascade comprising OC and *Pou2f2* transcription factors ensures proper distribution of V2 cells during spinal cord development. This program may not be restricted to V2 cells, as diversification and distribution of dorsal INs and of motor neurons are also altered in the absence of OC factors (Roy et al., 2012; Kabayiza et al., 2017) and as *Pou2f2* expression in the OC mutant spinal cord is increased in multiple neuronal populations.

MATERIALS AND METHODS

Ethics Statement and Mouse Lines

All experiments were strictly performed in accordance with the European Community Council directive of November 24, 1986 (86-609/ECC) and the decree of October 20, 1987 (87-848/EEC). Mice were raised in our animal facilities and treated according to the principles of laboratory animal care, and experiments and mouse housing were approved by the Animal Welfare Committee of Université catholique de Louvain (Permit Number: 2013/UCL/MD/11 and 2017/UCL/MD/008). The day of vaginal plug was considered to be embryonic day (e) 0.5. A minimum of three embryos of the same genotype was analyzed in each experiment. The embryos were collected at e12.5 and e14.5. The *Hnf6;Oc2* and the *Pou2f2* mutant mice were previously described (Corcoran et al., 1993; Jacquemin et al., 2000; Clotman et al., 2005). In the *Hnf6^{-/-}Oc2^{-/-}* embryos, expression of *Oc3* is completely downregulated in the developing spinal cord (Roy et al., 2012; Kabayiza et al., 2017), enabling to study spinal cord development in the absence of the three OC factors. The mice and the embryos were genotyped by PCR (primer information available on request).

In situ Hybridization (ISH) and Immunofluorescence Labelings

For ISH, the collected embryos were fixed in ice-cold 4% paraformaldehyde (PFA) in phosphate buffered-saline (PBS) overnight at 4°C, washed thrice in PBS for 10 min, incubated in PBS/30% sucrose solution overnight at 4°C, embedded and frozen in PBS/15% sucrose/7.5% gelatin. Fourteen μ m section were prepared and ISH was performed as previously described (Beguín et al., 2013; Pelosi et al., 2014; Francius et al., 2016) with DIG-conjugated *Pou2f2* (NM_011138.1, nucleotides 604-1187) or *Pou2f2* exon 5b (XM_006539651.3, nucleotides 643-876) antisense RNA probes. Control and *Onecut* mutant sections were placed adjacent on the same histology slides to minimize inter-slide variations in ISH signals.

For immunofluorescence, collected embryos were fixed in 4% PFA/PBS for 25 or 35 min according to their embryonic stage and processed as for ISH. Immunolabeling was performed on 14 μ m serial cryosections as previously described (Francius and Clotman, 2010). Primary antibodies against the following proteins were used: Chx10 (sheep; 1:500; Exalpha Biologicals #X1179P), Foxp1 (goat; 1:1000; R&D Systems #AF4534), Gata3 (rat; 1:50; Absea Biotechnology #11214D02), GFP (chick; 1:1000; Aves Lab #GFP-1020), HNF6 (guinea pig; 1:2000; (España and Clotman, 2012b); or rabbit; 1:100; Santa Cruz #sc-13050; or sheep; 1:1000 R&D Systems #AF6277), cMaf (rabbit; 1:3000; kindly provided by H. Wende), MafA (guinea pig; 1:500; kindly provide by T. Müller), OC2 (rat; 1:400; (Clotman et al., 2005); or sheep; 1:500; R&D Systems #AF6294), OC3 [guinea pig; 1:6000; (Pierreux et al., 2004)], *Pou2f2* (rabbit; 1:2000; Abcam #ab178679), *Shox2* (mouse; 1:500; Abcam #ab55740), *Sox1* (goat; 1:500; Santa Cruz #sc-17318). Secondary antibodies donkey anti-guinea pig/AlexaFluor 488, 594 or 647, anti-mouse/AlexaFluor 488, 594, or 647, anti-rabbit/AlexaFluor 594 or 647, anti-goat/AlexaFluor 488, anti-rat/AlexaFluor 647, anti-sheep/AlexaFluor 594 or 647, and goat anti-mouse IgG2A specific/AlexiaFluor 488, purchased from ThermoFisher Scientific or Jackson Laboratories were used at dilution 1:2000 or 1:1000, respectively.

In ovo Electroporation

In ovo electroporations were performed at stage HH14-16, as previously described (Roy et al., 2012). The coding sequence of the *S_Pou2f2.4* transcript was amplified by overlapping-PCR using: forward 5' GCTCTGTCTGCCCAAGAGAAA 3' and reverse 5' GTTGGGACAAGGTGAGCTGT 3' primers for the 5' sequence, forward 5' CCACCATCACAGCCTACCAG 3' and reverse 5' ATTATCTCGAGCCAGCCTCCTTACCCTCTCT 3' (designed to enable integration at the *XhoI* restriction site of the pCMV-MCS vector) primers for the 3' sequence. This sequence was first subcloned in a pCR[®]II-Topo[®] vector (Life Technologies, 45-0640) for sequencing then subcloned at the *EcoRI* (from the pCR[®]II-Topo[®] vector) and *XhoI* restriction sites of a pCMV-MCS vector for the *in ovo* electroporation. The pCMV-*Pou2f2* (0.5 μ g/ml) vector was co-electroporated with a pCMV-eGFP plasmid (0.25 μ g/ml) to visualize electroporated cells. The embryos were collected 72 h

(HH27-28) after electroporation, fixed in PBS/4%PFA for 45 min and processed for immunofluorescence labelings as previously described (Francius and Clotman, 2010). The thoracic region of the electroporated spinal cord was used for analyzes. To minimize stage and experimental condition variations, the non-electroporated side of the spinal cord was used as control for quantification and distribution analyses.

Imaging and Quantitative Analyses

Immunofluorescence and ISH images of cryosections were acquired on an EVOS FL Auto Imaging System (Thermo Fisher Scientific) or a Confocal laser Scanning biological microscope FV1000 Fluoview with the FV10-ASW 01.02 software (Olympus). The images were processed with Adobe Photoshop CS5 software to match brightness and contrast with the observation. Quantifications were performed by subtractive method (Francius and Clotman, 2010). For each embryo ($n \geq 3$), one side of three to five sections at brachial, thoracic, or lumbar level were quantified using the count analysis tool of Adobe Photoshop CS5 software. Raw data were exported from Adobe Photoshop CS5 software to Sigma Plotv12.3 software to perform statistical analyses. The histograms were drawn with Microsoft Excel. Adequate statistical tests (standard Student's t -tests or Mann-Whitney U tests) were applied depending on the number of comparisons and on the variance in each group. Quantitative analyses were considered significant at $p \leq 0.05$.

Quantitative analyzes of IN spatial distribution were performed as previously described (Kabayiza et al., 2017). Statistical analyses of ventral IN distribution were performed using a two-sample Hotelling's T^2 , which is a two-dimensional generalization of the Student's t -test. The analysis was implemented using the NCSS software package.

Microarray Analyses

RNA was extracted from control or *Hnfb6/Oc2* double-mutant spinal cords. The tissue was manually dissociated in Tripur isolation reagent (Roche, 11 667 165 001). After dissociation, chloroform (Merck Millipore, 1 02445 1000) was added to the sample, incubated at room temperature for 10 min and centrifugated for 10 min at 4°C. The aqueous phase was collected and the RNA was precipitated with isopropanol (VWR, 20880.310) and centrifugated for 15 min at 4°C. The pellet was washed in ethanol (Biosolve, 06250502) and centrifugated for 10 min at 4°C. The dried pellet was resuspended in RNase free water. The integrity of the RNA was assessed using an Agilent RNA 6000 Nano assay procedure. For microarray analyzes, the RNA was converted in single-strand cDNA, labeled using the GeneChip® WT PLUS Reagent Kit (Affymetrix) and hybridized on the GeneChip® MoGene 2.0 ST array (Affymetrix, 90 2118) using Affymetrix devices: Genechip® Fluidics Station 450, Genechip® Hybridization oven 640, Affymetrix Genechip® scanner and the Expression Consol software. The analyzes were performed using the R software. Microarray data have been deposited in the GEO repository (accession number: GSE117871).

Amplification of *Pou2f2* Isoforms and Sequencing

Fragments of the different *Pou2f2* isoforms were amplified by RT-PCR from RNA of control B lymphocytes or embryonic spinal cords purified as described above using the iScript™ Reverse transcriptase and the 5x iScript™ reaction mix (BioRad). *Pou2f2* sequences (Table 2) were amplified using a GoTaq® Green master mix (Promega, M712) or a Q5® Hot Start High-Fidelity DNA Polymerase (New England BioLabs® Inc., M0493S) (primer information available on request). Sequencing of the spinal *Pou2f2* exons was outsourced to Genewiz.

Quantitative real-time PCR was performed on 1/100 of the retrotranscription reaction using iTaq™ universal SYBR® Green Supermix (BioRad, 172-5124) on a CFX Connect™ Real-Time System (BioRad) with the BioRad CFX Manage 3.1 software. Each reaction was performed in duplicate and relative mRNA quantities were normalized to the housekeeping gene RPL32 (primer information available on request). Relative expression changes between conditions were calculated using the $\Delta\Delta Ct$ method. All changes are shown as fold changes.

AUTHOR CONTRIBUTIONS

AH, GM, CF, and FC designed the experiments. BJ generated Matlab routines for the distribution analyses of dorsal interneurons. LC provided *Pou2f2*^{+/-} sperm to generate the *Pou2f2* mutant mouse line. AH, GM, AC, MT, MH-F, and CF performed the experiments. All the authors discussed the data. AH and FC drafted the manuscript.

FUNDING

Work in the FC laboratory was supported by grants from the “Fonds spéciaux de recherche” (FSR) of the Université catholique de Louvain, by a “Projet de recherche (PDR)” #T.0117.13 and an “Equipement (EQP)” funding #U.N027.14 of the Fonds de la Recherche Scientifique (F.R.S.-FNRS, Belgium), by the “Actions de Recherche Concertées (ARC)” #10/15-026 and #17/22-079 of the “Direction générale de l'Enseignement non obligatoire et de la Recherche scientifique – Direction de la Recherche scientifique – Communauté française de Belgique” and granted by the “Académie Universitaire ‘Louvain’ and by the Association Belge contre les Maladies Neuro-Musculaires. LC acknowledges funding from the Australian Government (NHMRC IRIIS and research grants #637306 and #575500) and Victorian State Government Operational Infrastructure Support. AH and GM hold Ph.D. grants from the Fonds pour la Recherche dans l'Industrie et l'Agriculture (F.R.S.-FNRS, Belgium). MH-F was a Postdoctoral Researcher of the F.R.S.-FNRS. FC is a Senior Research Associate of the F.R.S.-FNRS.

ACKNOWLEDGMENTS

We thank members of the NEDI lab for material, technical support, and discussions. We are grateful to Drs. T. Müller and

H. Wende for kindly providing the guinea pig anti MafA and the rabbit anti cMaf antibodies, respectively, to Drs. F. Lemaigre and P. Jacquemin for the *Hnf6/Oc2* double mutant mice, to Dr. C. Pierreux for the pCMV-MCS, to Dr. J. Ambroise for assistance with the microarray analyses, and to Dr. L. Dumoutier for cDNA of B lymphocytes. This manuscript has been released as a Pre-Print at BioRxiv (Harris et al., 2018).

SUPPLEMENTARY MATERIAL

The Supplementary Material for this article can be found online at: <https://www.frontiersin.org/articles/10.3389/fncel.2019.00184/full#supplementary-material>

FIGURE S1 | Onecut factors regulate the diversification of the V2 interneurons. **(A–H’)** Immunolabelings of the V2a generic marker Chx10 and markers of V2a subpopulations on transverse spinal cord sections (brachial or thoracic levels) control or *Hnf6*^{-/-};*Oc2*^{-/-} mutant embryos at e14.5. Quantifications are shown in **Figure 1**. V2a **(A,B)**, Shox2+ V2a (arrows) and V2d interneurons **(C–D’)**, arrowheads are present in both control and double mutant embryos. **(E–E’)** MafA is present in a V2a subpopulation in control embryos (arrows), **(F–F’)** but is not detected in Chx10+ cells in the absence of OC factors. **(G–G’)** Similarly, cMaf is present in a subpopulation of V2a interneurons in control embryos (arrows), **(H–H’)** which is not the case in *Hnf6*^{-/-};*Oc2*^{-/-} embryos. **(I–L’)** Immunolabelings of the V2b generic marker Gata3 and the marker of V2b subpopulation, MafA. V2b **(I–J’)** and MafA+ V2b **(K–L’)**, arrows interneurons are present in control and in *Hnf6*^{-/-};*Oc2*^{-/-} embryos. **(M,N)** The number of V2c interneurons is unchanged is similarly detected in *Hnf6*^{-/-};*Oc2*^{-/-} embryos as compared to control embryos (delineated cells). Sox1 in the ventricular zone labels neural progenitors. Scale bar = 50 μm.

FIGURE S2 | *Pou2f2* RT-PCR experiments and sequencing of exon 1b and exon 5b of the spinal *Pou2f2* isoforms. Composite assembly of electrophoresis images of RT-PCR amplification products for *Pou2f2* isoform sequences on embryonic spinal cord or B-cell RNA samples. Water was used as a negative control (Ctl-). **(A)** Amplifications from exon 1 (E1) to E6 on embryonic spinal cord RNA samples (asterisk) fail to amplify the RNA isoforms detected in B cell samples. In contrast, amplifications from E7 to E9, from E10 to E12, and from E13 to E17 show at least one similar amplicon in spinal cord samples and in B cell samples. **(B)** Amplification from E1 (other forward primer) to E7 also fails to amplify *Pou2f2*

spinal cord isoforms. In contrast, amplifications from E2, 3, 4, and 5 to E7 produce systematically longer amplicons in spinal cord samples (arrowheads) as compared to B cell samples. The E6 to E7 amplification is similar in both samples. **(C)** Amplifications from E1X (present in the X6 sequence) to E3 do not produce amplicon in B-cell samples (asterisk). Amplifications from E1X to E3 or to E5b on spinal cord samples systematically produce two amplicons (arrowheads). Amplifications of the E5b exon sequence, from E3 to E5b and from E5b to E7 produce expected amplicons in spinal cord samples. **(D)** Comparison of exon 1b and exon 5b sequences in the predicted X6 sequence and the sequenced embryonic spinal cord *Pou2f2* isoforms. Sequences of E1X, E2a, and E5b exons align (100% identity) with the predicted X6 sequence. Sequence of the additional alternative exon 1b is shown. SD, size standard; E, exon; SC, embryonic spinal cord; B, B lymphocytes.

FIGURE S3 | The number of *Pou2f2*+*Shox2*+ V2a interneurons is normal in *Hnf6*^{-/-};*Oc2*^{-/-} mutant embryos. Immunolabelings on transverse spinal cord sections (brachial or thoracic levels) of control or *Hnf6*^{-/-};*Oc2*^{-/-} mutant embryos. At e12.5 **(A–C)** and at e14.5 **(D–F)**, the number of V2a containing *Shox2* and *Pou2f2* is unchanged in the absence of OC factors. Mean values ± SEM. Scale bar = 50 μm.

FIGURE S4 | Efficacy of pCMV-eGFP and pCMV-*Pou2f2* co-electroporation in the chicken embryonic spinal cord. **(A–C)** eGFP (green, **B**), and *Pou2f2* (red, **C**) are present in a vast majority of cells along the dorso-ventral axis of the spinal cord. Scale bar = 50 μm.

FIGURE S5 | The number of MafA+ or cMaf+ V2a interneurons is normal in *Pou2f2*^{-/-} mutant spinal cords. Immunolabelings on transverse spinal cord sections (brachial or thoracic levels) of control or *Pou2f2*^{-/-} mutant embryos at e12.5. **(A–F)** Absence of *Pou2f2* does not impact on the number of *Shox2*+ **(A–C)**, cMaf+ **(D–F)**, or MafA+ **(G–I)** V2a interneurons. Mean values ± SEM. Scale bar = 50 μm.

FIGURE S6 | The number of MafA-positive V2b interneurons or of the V2c interneurons is normal in *Pou2f2*^{-/-} mutant spinal cords. Immunolabelings on transverse spinal cord sections (brachial or thoracic levels) of control or *Pou2f2*^{-/-} mutant embryos at e12.5. **(A,B,E)** The number of MafA+ V2b interneurons is not significantly altered in the absence of *Pou2f2*. **(C,D,F)** Similarly, the production of V2c interneurons is not affected in *Pou2f2* mutants. Mean values ± SEM. Scale bar = 50 μm.

TABLE S1 | Microarray comparison of control and of *Hnf6*^{-/-};*Oc2*^{-/-} spinal cords. The differential expression of selected candidates is shown as fold change in *Hnf6*^{-/-};*Oc2*^{-/-} vs. control spinal cords. Pval, *p*-value; adjpval, adjusted *p*-value.

REFERENCES

- Ampatzis, K., Song, J., Ausborn, J., and El Manira, A. (2014). Separate microcircuit modules of distinct v2a interneurons and motoneurons control the speed of locomotion. *Neuron* 83, 934–943. doi: 10.1016/j.neuron.2014.07.018
- Audouard, E., Schakman, O., Ginion, A., Bertrand, L., Gailly, P., and Clotman, F. (2013). The Onecut transcription factor HNF-6 contributes to proper reorganization of Purkinje cells during postnatal cerebellum development. *Mol. Cell. Neurosci.* 56, 159–168. doi: 10.1016/j.mcn.2013.05.001
- Audouard, E., Schakman, O., Rene, F., Huettl, R. E., Huber, A. B., Loeffler, J. P., et al. (2012). The Onecut transcription factor HNF-6 regulates in motor neurons the formation of the neuromuscular junctions. *PLoS One* 7:e50509. doi: 10.1371/journal.pone.0050509
- Barber, M., and Pierani, A. (2016). Tangential migration of glutamatergic neurons and cortical patterning during development: lessons from Cajal-Retzus cells. *Dev. Neurobiol.* 76, 847–881. doi: 10.1002/dneu.22363
- Beaudry, J. B., Pierreux, C. E., Hayhurst, G. P., Plumb-Rudewicz, N., Weiss, M. C., Rousseau, G. G., et al. (2006). Threshold levels of hepatocyte nuclear factor 6 (HNF-6) acting in synergy with HNF-4 and PGC-1alpha are required for time-specific gene expression during liver development. *Mol. Cell. Biol.* 26, 6037–6046. doi: 10.1128/MCB.02445-05
- Beguini, S., Crepel, V., Aniksztejn, L., Becq, H., Pelosi, B., Pallesi-Pocachard, E., et al. (2013). An epilepsy-related ARX polyalanine expansion modifies glutamatergic neurons excitability and morphology without affecting GABAergic neurons development. *Cereb. Cortex* 23, 1484–1494. doi: 10.1093/cercor/bhs138
- Bikoff, J. B., Gabitto, M. I., Rivard, A. F., Drobac, E., Machado, T. A., Miri, A., et al. (2016). Spinal inhibitory interneuron diversity delineates variant motor microcircuits. *Cell* 165, 207–219. doi: 10.1016/j.cell.2016.01.027
- Blacklaws, J., Deska-Gauthier, D., Jones, C. T., Petracca, Y. L., Liu, M., Zhang, H., et al. (2015). Sim1 is required for the migration and axonal projections of V3 interneurons in the developing mouse spinal cord. *Dev. Neurobiol.* 75, 1003–1017. doi: 10.1002/dneu.22266
- Boije, H., and Kullander, K. (2018). Origin and circuitry of spinal locomotor interneurons generating different speeds. *Curr. Opin. Neurobiol.* 53, 16–21. doi: 10.1016/j.comb.2018.04.024
- Borowska, J., Jones, C. T., Deska-Gauthier, D., and Zhang, Y. (2015). V3 interneuron subpopulations in the mouse spinal cord undergo distinctive postnatal maturation processes. *Neuroscience* 295, 221–228. doi: 10.1016/j.neuroscience.2015.03.024
- Borowska, J., Jones, C. T., Zhang, H., Blacklaws, J., Goulding, M., and Zhang, Y. (2013). Functional subpopulations of V3 interneurons in the mature mouse spinal cord. *J. Neurosci.* 33, 18553–18565. doi: 10.1523/JNEUROSCI.2005-13.2013

- Britz, O., Zhang, J., Grossmann, K. S., Dyck, J., Kim, J. C., Dymecki, S., et al. (2015). A genetically defined asymmetry underlies the inhibitory control of flexor-extensor locomotor movements. *eLife* 4:e04718. doi: 10.7554/eLife.04718
- Camos, S., Gubern, C., Sobrado, M., Rodriguez, R., Romera, V. G., Moro, M. A., et al. (2014). Oct-2 transcription factor binding activity and expression up-regulation in rat cerebral ischaemia is associated with a diminution of neuronal damage in vitro. *Neuromol. Med.* 16, 332–349. doi: 10.1007/s12017-013-8279-1
- Catela, C., Shin, M. M., and Dasen, J. S. (2015). Assembly and function of spinal circuits for motor control. *Annu. Rev. Cell Dev. Biol.* 31, 669–698. doi: 10.1146/annurev-cellbio-100814-125155
- Clotman, F., Jacquemin, P., Plumb-Rudewicz, N., Pierreux, C. E., Van der Smissen, P., Dietz, H. C., et al. (2005). Control of liver cell fate decision by a gradient of TGF beta signaling modulated by onecut transcription factors. *Genes Dev.* 19, 1849–1854. doi: 10.1101/gad.340305
- Cloviss, Y. M., Seo, S. Y., Kwon, J. S., Rhee, J. C., Yeo, S., Lee, J. W., et al. (2016). Chx10 consolidates V2a interneuron identity through two distinct gene repression modes. *Cell Rep.* 16, 1642–1652. doi: 10.1016/j.celrep.2016.06.100
- Corcoran, L. M., Karvelas, M., Nossal, G. J., Ye, Z. S., Jacks, T., and Baltimore, D. (1993). Oct-2, although not required for early B-cell development, is critical for later B-cell maturation and for postnatal survival. *Genes Dev.* 7, 570–582. doi: 10.1101/gad.7.4.570
- Corcoran, L. M., Koentgen, F., Dietrich, W., Veale, M., and Humbert, P. O. (2004). All known in vivo functions of the Oct-2 transcription factor require the C-terminal protein domain. *J. Immunol.* 172, 2962–2969. doi: 10.4049/jimmunol.172.5.2962
- Crone, S. A., Quinlan, K. A., Zagoraiou, L., Droho, S., Restrepo, C. E., Lundfald, L., et al. (2008). Genetic ablation of V2a ipsilateral interneurons disrupts left-right locomotor coordination in mammalian spinal cord. *Neuron* 60, 70–83. doi: 10.1016/j.neuron.2008.08.009
- Del Barrio, M. G., Taveira-Marques, R., Muroyama, Y., Yuk, D. I., Li, S., Wines-Samuelson, M., et al. (2007). A regulatory network involving Foxn4, Mash1 and delta-like 4/Notch1 generates V2a and V2b spinal interneurons from a common progenitor pool. *Development* 134, 3427–3436. doi: 10.1242/dev.005868
- Dougherty, K. J., and Kiehn, O. (2010). Firing and cellular properties of V2a interneurons in the rodent spinal cord. *J. Neurosci.* 30, 24–37. doi: 10.1523/JNEUROSCI.4821-09.2010
- Dougherty, K. J., Zagoraiou, L., Satoh, D., Rozani, I., Doobar, S., Arber, S., et al. (2013). Locomotor rhythm generation linked to the output of spinal shox2 excitatory interneurons. *Neuron* 80, 920–933. doi: 10.1016/j.neuron.2013.08.015
- Espana, A., and Clotman, F. (2012a). Onecut factors control development of the Locus Coeruleus and of the mesencephalic trigeminal nucleus. *Mol. Cell. Neurosci.* 50, 93–102. doi: 10.1016/j.mcn.2012.04.002
- Espana, A., and Clotman, F. (2012b). Onecut transcription factors are required for the second phase of development of the A13 dopaminergic nucleus in the mouse. *J. Comp. Neurol.* 520, 1424–1441. doi: 10.1002/cne.22803
- Francius, C., and Clotman, F. (2010). Dynamic expression of the onecut transcription factors HNF-6, OC-2 and OC-3 during spinal motor neuron development. *Neuroscience* 165, 116–129. doi: 10.1016/j.neuroscience.2009.09.076
- Francius, C., and Clotman, F. (2014). Generating spinal motor neuron diversity: a long quest for neuronal identity. *Cell. Mol. Life Sci.* 71, 813–829. doi: 10.1007/s00018-013-1398-x
- Francius, C., Harris, A., Rucchin, V., Hendricks, T. J., Stam, F. J., Barber, M., et al. (2013). Identification of multiple subsets of ventral interneurons and differential distribution along the rostrocaudal axis of the developing spinal cord. *PLoS One* 8:e70325. doi: 10.1371/journal.pone.0070325
- Francius, C., Hidalgo-Figueroa, M., Debrulle, S., Pelosi, B., Rucchin, V., Ronellenfitch, K., et al. (2016). Vsx1 transiently defines an early intermediate V2 interneuron precursor compartment in the mouse developing spinal cord. *Front. Mol. Neurosci.* 9:145. doi: 10.3389/fnmol.2016.00145
- Goetz, C., Pivetta, C., and Arber, S. (2015). Distinct limb and trunk premotor circuits establish laterality in the spinal cord. *Neuron* 85, 131–144. doi: 10.1016/j.neuron.2014.11.024
- Gosgnach, S., Bikoff, J. B., Dougherty, K. J., El Manira, A., Lanuza, G. M., and Zhang, Y. (2017). Delineating the diversity of spinal interneurons in locomotor circuits. *J. Neurosci.* 37, 10835–10841. doi: 10.1523/JNEUROSCI.1829-17.2017
- Grossmann, K. S., Giraudin, A., Britz, O., Zhang, J., and Goulding, M. (2010). Genetic dissection of rhythmic motor networks in mice. *Prog. Brain Res.* 187, 19–37. doi: 10.1016/B978-0-444-53613-6.00002-2
- Guo, J., and Anton, E. S. (2014). Decision making during interneuron migration in the developing cerebral cortex. *Trends Cell Biol.* 24, 342–351. doi: 10.1016/j.tcb.2013.12.001
- Harris, A., Masgutova, G., Collin, A., Toch, M., Hidalgo-Figueroa, M., Jacob, B., et al. (2018). Onecut factors and Pou2f2 regulate the distribution of V2 interneurons in the mouse developing spinal cord. *bioRxiv* [Preprint]. doi: 10.1101/413054
- Hatzopoulos, A. K., Stoykova, A. S., Erselius, J. R., Goulding, M., Neuman, T., and Gruss, P. (1990). Structure and expression of the mouse Oct2a and Oct2b, two differentially spliced products of the same gene. *Development* 109, 349–362.
- Hayashi, M., Hinkley, C. A., Driscoll, S. P., Moore, N. J., Levine, A. J., Hilde, K. L., et al. (2018). Graded arrays of spinal and supraspinal V2a interneuron subtypes underlie forelimb and hindlimb motor control. *Neuron* 97, 869–884.e5. doi: 10.1016/j.neuron.2018.01.023
- Hilde, K. L., Levine, A. J., Hinkley, C. A., Hayashi, M., Montgomery, J. M., Gullo, M., et al. (2016). Satb2 is required for the development of a spinal exteroceptive microcircuit that modulates limb position. *Neuron* 91, 763–776. doi: 10.1016/j.neuron.2016.07.014
- Hodson, D. J., Shaffer, A. L., Xiao, W., Wright, G. W., Schmitz, R., Phelan, J. D., et al. (2016). Regulation of normal B-cell differentiation and malignant B-cell survival by OCT2. *Proc. Natl. Acad. Sci. U.S.A.* 113, E2039–E2046. doi: 10.1073/pnas.1600557113
- Jacquemin, P., Durvieux, S. M., Jensen, J., Godfraind, C., Gradwohl, G., Guillemot, F., et al. (2000). Transcription factor hepatocyte nuclear factor 6 regulates pancreatic endocrine cell differentiation and controls expression of the proendocrine gene *ngn3*. *Mol. Cell. Biol.* 20, 4445–4454. doi: 10.1128/mcb.20.12.4445-4454.2000
- Jacquemin, P., Lannoy, V. J., Rousseau, G. G., and Lemaigre, F. P. (1999). OC-2, a novel mammalian member of the ONECUT class of homeodomain transcription factors whose function in liver partially overlaps with that of hepatocyte nuclear factor-6. *J. Biol. Chem.* 274, 2665–2671. doi: 10.1074/jbc.274.5.2665
- Jacquemin, P., Lemaigre, F. P., and Rousseau, G. G. (2003a). The onecut transcription factor HNF-6 (OC-1) is required for timely specification of the pancreas and acts upstream of Pdx-1 in the specification cascade. *Dev. Biol.* 258, 105–116. doi: 10.1016/S0012-1606(03)00115-5
- Jacquemin, P., Pierreux, C. E., Fierens, S., van Eyll, J. M., Lemaigre, F. P., and Rousseau, G. G. (2003b). Cloning and embryonic expression pattern of the mouse onecut transcription factor OC-2. *Gene Expr. Patterns* 3, 639–644. doi: 10.1016/S1567-133X(03)00110-8
- Joshi, K., Lee, S., Lee, B., Lee, J. W., and Lee, S. K. (2009). LMO4 controls the balance between excitatory and inhibitory spinal V2 interneurons. *Neuron* 61, 839–851. doi: 10.1016/j.neuron.2009.02.011
- Kabayiza, K. U., Masgutova, G., Harris, A., Rucchin, V., Jacob, B., and Clotman, F. (2017). The onecut transcription factors regulate differentiation and distribution of dorsal interneurons during spinal cord development. *Front. Mol. Neurosci.* 10:157. doi: 10.3389/fnmol.2017.00157
- Konig, H., Pfisterer, P., Corcoran, L. M., and Wirth, T. (1995). Identification of CD36 as the first gene dependent on the B-cell differentiation factor Oct-2. *Genes Dev.* 9, 1598–1607. doi: 10.1101/gad.9.13.1598
- Lai, H. C., Seal, R. P., and Johnson, J. E. (2016). Making sense out of spinal cord somatosensory development. *Development* 143, 3434–3448. doi: 10.1242/dev.139592
- Landry, C., Clotman, F., Hioki, T., Oda, H., Picard, J. J., Lemaigre, F. P., et al. (1997). HNF-6 is expressed in endoderm derivatives and nervous system of the mouse embryo and participates to the cross-regulatory network of liver-enriched transcription factors. *Dev. Biol.* 192, 247–257. doi: 10.1006/dbio.1997.8757
- Lannoy, V. J., Rodolosse, A., Pierreux, C. E., Rousseau, G. G., and Lemaigre, F. P. (2000). Transcriptional stimulation by hepatocyte nuclear factor-6. Target-specific recruitment of either CREB-binding protein (CBP) or p300/CBP-associated factor (p/CAF). *J. Biol. Chem.* 275, 22098–22103. doi: 10.1074/jbc.M000855200
- Latchman, D. S. (1996). The Oct-2 transcription factor. *Int. J. Biochem. Cell Biol.* 28, 1081–1083.

- Lee, S., Lee, B., Joshi, K., Pfaff, S. L., Lee, J. W., and Lee, S. K. (2008). A regulatory network to segregate the identity of neuronal subtypes. *Dev. Cell* 14, 877–889. doi: 10.1016/j.devcel.2008.03.021
- Lemaigre, F. P., Durviaux, S. M., Truong, O., Lannoy, V. J., Hsuan, J. J., and Rousseau, G. G. (1996). Hepatocyte nuclear factor 6, a transcription factor that contains a novel type of homeodomain and a single cut domain. *Proc. Natl. Acad. Sci. U.S.A.* 93, 9460–9464. doi: 10.1073/pnas.93.18.9460
- Lillycrop, K. A., and Latchman, D. S. (1992). Alternative splicing of the Oct-2 transcription factor RNA is differentially regulated in neuronal cells and B cells and results in protein isoforms with opposite effects on the activity of octamer/TAATGARAT-containing promoters. *J. Biol. Chem.* 267, 24960–24965.
- Liu, Y. Z., Lillycrop, K. A., and Latchman, D. S. (1995). Regulated splicing of the Oct-2 transcription factor RNA in neuronal cells. *Neurosci. Lett.* 183, 8–12. doi: 10.1016/0304-3940(94)11102-o
- Lu, D. C., Niu, T., and Alaynick, W. A. (2015). Molecular and cellular development of spinal cord locomotor circuitry. *Front. Mol. Neurosci.* 8:25. doi: 10.3389/fnmol.2015.00025
- Misra, K., Luo, H., Li, S., Matisse, M., and Xiang, M. (2014). Asymmetric activation of Dll4-Notch signaling by Foxn4 and proneural factors activates BMP/TGFbeta signaling to specify V2b interneurons in the spinal cord. *Development* 141, 187–198. doi: 10.1242/dev.092536
- Panayi, H., Panayiotou, E., Orford, M., Genethliou, N., Mean, R., Lapatitis, G., et al. (2010). Sox1 is required for the specification of a novel p2-derived interneuron subtype in the mouse ventral spinal cord. *J. Neurosci.* 30, 12274–12280. doi: 10.1523/JNEUROSCI.2402-10.2010
- Pelosi, B., Migliarini, S., Pacini, G., Pratelli, M., and Pasqualetti, M. (2014). Generation of Pet1210-Cre transgenic mouse line reveals non-serotonergic expression domains of Pet1 both in CNS and periphery. *PLoS One* 9:e104318. doi: 10.1371/journal.pone.0104318
- Peng, C. Y., Yajima, H., Burns, C. E., Zon, L. I., Sisodia, S. S., Pfaff, S. L., et al. (2007). Notch and MAML signaling drives Scl-dependent interneuron diversity in the spinal cord. *Neuron* 53, 813–827. doi: 10.1016/j.neuron.2007.02.019
- Pierreux, C. E., Vanhorenbeeck, V., Jacquemin, P., Lemaigre, F. P., and Rousseau, G. G. (2004). The transcription factor hepatocyte nuclear factor-6/Onecut-1 controls the expression of its paralog Onecut-3 in developing mouse endoderm. *J. Biol. Chem.* 279, 51298–51304. doi: 10.1074/jbc.M409038200M409038200
- Roy, A., Francius, C., Rouso, D. L., Seuntjens, E., Debruyne, J., Luxenhofer, G., et al. (2012). Onecut transcription factors act upstream of Isl1 to regulate spinal motoneuron diversification. *Development* 139, 3109–3119. doi: 10.1242/dev.078501
- Stam, F. J., Hendricks, T. J., Zhang, J., Geiman, E. J., Francius, C., Labosky, P. A., et al. (2012). Renshaw cell interneuron specialization is controlled by a temporally restricted transcription factor program. *Development* 139, 179–190. doi: 10.1242/dev.071134
- Stoykova, A. S., Sterrer, S., Erselius, J. R., Hatzopoulos, A. K., and Gruss, P. (1992). Mini-Oct and Oct-2c: two novel, functionally diverse murine Oct-2 gene products are differentially expressed in the CNS. *Neuron* 8, 541–558. doi: 10.1016/0896-6273(92)90282-i
- Surmeli, G., Akay, T., Ippolito, G. C., Tucker, P. W., and Jessell, T. M. (2011). Patterns of spinal sensory-motor connectivity prescribed by a dorsoventral positional template. *Cell* 147, 653–665. doi: 10.1016/j.cell.2011.10.012
- Sweeney, L. B., Bikoff, J. B., Gabitto, M. I., Brenner-Morton, S., Baek, M., Yang, J. H., et al. (2018). Origin and segmental diversity of spinal inhibitory interneurons. *Neuron* 97, 341–355.e3. doi: 10.1016/j.neuron.2017.12.029
- Talpal, A. E., Bouvier, J., Borgius, L., Fortin, G., Pierani, A., and Kiehn, O. (2013). Dual-mode operation of neuronal networks involved in left-right alternation. *Nature* 500, 85–88. doi: 10.1038/nature12286
- Thaler, J. P., Lee, S. K., Jurata, L. W., Gill, G. N., and Pfaff, S. L. (2002). LIM factor Lhx3 contributes to the specification of motor neuron and interneuron identity through cell-type-specific protein-protein interactions. *Cell* 110, 237–249. doi: 10.1016/S0092-8674(02)00823-1
- Theodorou, E., Dalember, G., Heffelfinger, C., White, E., Weissman, S., Corcoran, L., et al. (2009). A high throughput embryonic stem cell screen identifies Oct-2 as a bifunctional regulator of neuronal differentiation. *Genes Dev.* 23, 575–588. doi: 10.1101/gad.1772509
- Tripodi, M., Stepien, A. E., and Arber, S. (2011). Motor antagonism exposed by spatial segregation and timing of neurogenesis. *Nature* 479, 61–66. doi: 10.1038/nature10538
- Vanhorenbeeck, V., Jacquemin, P., Lemaigre, F. P., and Rousseau, G. G. (2002). OC-3, a novel mammalian member of the ONECUT class of transcription factors. *Biochem. Biophys. Res. Commun.* 292, 848–854. doi: 10.1006/bbrc.2002.6760
- Wirth, T., Priess, A., Annweiler, A., Zwilling, S., and Oeler, B. (1991). Multiple Oct2 isoforms are generated by alternative splicing. *Nucleic Acids Res.* 19, 43–51. doi: 10.1093/nar/19.1.43
- Ziskind-Conhaim, L., and Hochman, S. (2017). Diversity of molecularly defined spinal interneurons engaged in mammalian locomotor pattern generation. *J. Neurophysiol.* 118, 2956–2974. doi: 10.1152/jn.00322.2017

Conflict of Interest Statement: The authors declare that the research was conducted in the absence of any commercial or financial relationships that could be construed as a potential conflict of interest.

Copyright © 2019 Harris, Masgutova, Collin, Toch, Hidalgo-Figueroa, Jacob, Corcoran, Francius and Clotman. This is an open-access article distributed under the terms of the Creative Commons Attribution License (CC BY). The use, distribution or reproduction in other forums is permitted, provided the original author(s) and the copyright owner(s) are credited and that the original publication in this journal is cited, in accordance with accepted academic practice. No use, distribution or reproduction is permitted which does not comply with these terms.



Minerva Access is the Institutional Repository of The University of Melbourne

Author/s:

Harris, A; Masgutova, G; Collin, A; Toch, M; Hidalgo-Figueroa, M; Jacob, B; Corcoran, LM; Francius, C; Clotman, F

Title:

Onecut Factors and Pou2f2 Regulate the Distribution of V2 Interneurons in the Mouse Developing Spinal Cord

Date:

2019-06-05

Citation:

Harris, A., Masgutova, G., Collin, A., Toch, M., Hidalgo-Figueroa, M., Jacob, B., Corcoran, L. M., Francius, C. & Clotman, F. (2019). Onecut Factors and Pou2f2 Regulate the Distribution of V2 Interneurons in the Mouse Developing Spinal Cord. FRONTIERS IN CELLULAR NEUROSCIENCE, 13, <https://doi.org/10.3389/fncel.2019.00184>.

Persistent Link:

<http://hdl.handle.net/11343/249826>

File Description:

published version

License:

CC BY